OXIDATION OF SELECTED ORGANOSULFUR COMPOUNDS IN DODECANE OVER A HEATED METAL SURFACE

Robert E. Morris and George W. Mushrush

Chemistry Division, Code 6180
U.S. Naval Research Laboratory
Washington, D.C. 20375-5000

INTRODUCTION

The use of jet fuel as a heat exchange medium imposes significant levels of thermal stress. Hydrocarbon fuels subjected to such temperatures have been shown to undergo considerable degradation. This observed degradation can be manifested by the formation of deposits on heat exchanger surfaces, on filters, in nozzles and on combustor surfaces (1,2). Heteroatoms, i.e., oxygen, nitrogen and sulfur and ash have been found to comprise as much as 40 percent of such deposits (3).

Sulfur can constitute the most abundant heteroatom present in military jet fuel (JP-4 and JP-5), since up to 0.4% total sulfur by weight is allowed per MIL-T-5624M. In commercial jet fuels, the ASTM Standard Specification for Aviation Turbine Fuels (4) permits up to 0.3% total sulfur by weight. Trace levels of sulfur, particularly as thiols, have been found to greatly increase the deposit forming tendencies of fuels during thermal stress. For this reason, much more stringent controls over thiol content are generally exercised. Deposits formed in jet fuel over the temparature range of 150 to 650°C in the presence of oxygen have been found to contain a much greater percentage of sulfur, up to a 100-fold increase, than that present in the fuel itself (1,5). The sulfur content of these deposits has been found to vary from 1 to 9% (6). The formation of such deposits has been attributed to the participation of mercaptans, sulfides and disulfides (7). Trace levels of thiols, sulfides and polysulfides were found to increase deposit formation even in deoxygenated jet fuels (7,8,9). In contrast, accelerated storage testing of fuels at 120-135°C indicated that while thiols promoted deposit formation, sulfides and disulfides exhibited inhibitory effects on deposition by decomposing peroxides (10).

Previous work in our laboratory has shown that aldehydes, thiols, sulfides and disulfides could be readily oxidized by hydroperoxides (11,12,13). During accelerated storage testing of a jet fuel at 65°C for four weeks, we have found (14) peroxide levels of 0.1 meq/kg. In the presence of 0.03% (w/w) sulfur from thiophenol, the accumulation of peroxides increased to 1.4 meq/kg. If the oxygen availability is limited but the temperature is sufficiently high, the hydroperoxide level will then be limited by free radical decomposition. In studies of the same jet fuel in our laboratory using a modified JFTOT apparatus, the maximum

hydroperoxide concentration reached after sparging with air for 15 min before stressing was 0.7 meq/kg; sparging with pure oxygen for a similar time before stressing raised the maximum hydroperoxide concentration to 2.8 meq/kg at 280°C.

It is difficult to identify specific reaction pathways from studies of fuels, which are complex mixtures. Model studies have been utilized to determine trace reaction products. These model studies were conducted in sealed borosilicate glass tubes at 120°C for up to 60 min. From the t-butylhydroperoxide (tBHP) initiated oxidation of dodecane thiol and hexyl sulfide (13) the major oxidation products were the dodecyl disulfide and hexyl sulfoxide, respectively. Similar studies revealed the major product of the oxidation of thiophenol by tBHP or oxygen to be phenyl disulfide.

We have utilized our modified JFTOT apparatus as a first step in determining the applicability of the findings from the model studies with changes occurring in aircraft fuel systems. This paper describes studies of the oxidation of thiophenol and hexyl disulfide in dodecane during stress in the JFTOT.

EXPERIMENTAL

Reagents. n-Hexyl disulfide and Thiophenol were obtained from Aldrich Chemical Co. They were distilled in vacuo to 99.9% purity before use. n-Dodecane (99% min.) was obtained from Phillips Petroleum Co. and was used without further purification.

Methods. Samples were thermally stressed in the modified JFTOT apparatus which has been described previously (15). The sulfur compound was blended into the dodecane in a glass vessel and aerated samples with dry air for 15 minutes, where applicable. To increase the heated surface area available and to reduce the steepness of the tube temperature profile, 304 stainless steel JFTOT heater tubes with five-inch heated sections were employed. The modified JFTOT apparatus permits sampling of stressed samples after passing over the heater tube and before returning to the reservoir (15). Procedures for determining the oxygen and hydroperoxide concentrations in the stressed dodecane have been described earlier (16). Product identification was obtained by combined GC/MS (EI mode). The GC/MS unit consisted of a Hewlett-Packard Model 5980 GC coupled to a Finnigan MAT ion trap detector. An all glass GC inlet system was used in combination with a 0.2mm x 50m OV-101 fused silica capillary column. A carrier gas flow of 1mL/min was used with an inlet split ration of 60:1. A temperature program with an initial hold at 70°C for 2 min, increasing at 6°C/min, with a final temperature of 240°C.

RESULTS AND DISCUSSION

The influence exerted by sulfur compounds in controlled testing is affected not only by the structure of the organosulfur compound but also by the stress regimen employed. In the JFTOT, the liquid

flows at a rate of approximately 3 ml/min. With the non-standard length JFTOT heater tubes employed in this study, the sample passes over the tube in approximately 28 sec. While the JFTOT does not simulate turbulent flow conditions such as those in the heat exchangers, it does however provide a relatively short reaction time under conditions of limiting oxygen availability.

As the dodecane comes in contact with the hot metal surface of the heater tube, reaction with oxygen leads to autoxidation and the formation of peroxy radicals. The ensuing propagation mechanism continues as long as the temperature is sufficient to produce more free radicals. In the JFTOT where the reaction time is relatively short, the available dissolved oxygen is not fully depleted until the tube temperature approaches 300°C. This is evident in the temperature profiles of oxygen (Fig. 1) and hydroperoxide concentrations (Fig. 2) measured in neat dodecane. The profiles indicate a correspondence between oxygen consumption and hydroperoxide concentrations. While some peroxidation occurs below 220°C, rapid oxidation ensues above that temperature. At temperatures exceeding approximately 280°C, the dodecyl hydroperoxide undergoes decomposition (15), which accounts for the decrease in concentration above that temperature.

The addition of 0.4% (w/w) sulfur from n-hexyl disulfide (HDS) suppressed peroxidation (Table I) by about 46% of the level attained in the neat fuel. Additions of 0.2% (w/w) sulfur from HDS resulted in suppression to approximately 68% that of the neat dodecane.

Table I. Hydroperoxide Concentrations Measured in Dodecane Containing Organosulfur Compounds as a Function of JFTOT Maximum Heater Tube Temperature

	Hydroperoxides, meq/kg				
Maximum Tube		Hexyl Disulfide		Thiophenol	
Temp., °C	neat	0.2% S	0.4% S	0.005% S	0.03% S
21-120	nd[a]	nd	nd	nd	nd
200	0.11	0.01	nd	nd	nd
240	2.15	1.09	1.50	0.13	nd
280	2.25	1.03	1.52	1.02	nd
320	1.60	0.36	nd	0.69	nd

[a]not detected, less than 0.01 meq/kg.

While a proportional response between HDS concentration and suppression of peroxidation was observed, it was far from quantitative, given the great excess of sulfur over the quantity of hydroperoxide formed in the neat dodecane. This is probably a consequence of the limitations imposed by the relatively short reaction time. The oxidation of disulfides in non-aqueous media has been reported (17) to proceed via successive coordination of oxygen

to the sulfur centers to produce the α-disulfone which cleaves to yield the sulfonic acid. Comparison of oxygen consumption profiles shown as a function of temperature in Fig. 1 reveal that direct oxidation by dissolved oxygen did not play a role in peroxide reduction. Therefore, the disulfide was reacting with dodecane autoxidation products to block the formation of hydroperoxides. Attempts to identify the oxidation products of hexyl disulfide in the JFTOT effluent were complicated by the low concentration of products and the difficulties experienced in detection. Future studies directed towards model studies of hexyl disulfide oxidation by t-butyl hydroperoxide are expected to provide information concerning product distributions and allow for optimization of detection procedures.

Thiophenol was much more reactive and completely suppressed peroxidation when added at 0.03% (w/w) Sulfur (Table I). By reducing the amount of sulfur from thiophenol to 0.005% (w/w), a detectable amount of hydroperoxides accumulated at temperatures between 240 and 280°C. Previous model studies in our laboratory (13), have shown that the oxidation of thiophenol by t-BHP results in the formation of the corresponding disulfide, phenyl disulfide. The oxidation of thiols classically occurs through the formation of the thiyl radical, which in the case of thiophenol, would be favored by resonance stabilization through the phenyl group. Thus, it is not surprising that thiophenol would be such an effective radical trap, terminating the chain reactions early in the propagation step. Examination of the oxygen consumption profiles generated from dodecane containing 0.03% and 0.005% (w/w) sulfur from thiophenol confirm that the free radical chain reactions were being terminated very quickly before significant autoxidation could ensue. In the presence of thiophenol, the oxygen consumption was reduced with respect to that of the neat dodecane.

Examination of the reaction products of thiophenol oxidation in the JFTOT by combined GC/MS confirmed the presence of phenyl disulfide. Examination of JFTOT effluent taken over a range of temperatures by GC/MS (Fig. 2) revealed that the formation of the disulfide corresponded to the temperature at which dodecane autoxidation proceeded and the hydroperoxide concentration in the neat dodecane reached a maximum. Thus thiophenol was being oxidized to the phenyl disulfide by dodecane autoxidation products, most likely by dodecoxy radicals, which suppressed the formation of hydroperoxides. The conversion to phenyl disulfide reached a maximum at temperatures above 300°C, which corresponds to the temperature at which all the available oxygen has been consumed and where dodecyl hydroperoxide disproportionates. To determine the contribution of the anaerobic thermal decomposition of the thiophenol to thiyl radicals and dimerization to phenyl disulfide, deoxygenated dodecane containing 0.03% (w/w) sulfur from thiophenol was examined. The corresponding curve (Fig. 2) for disulfide/thiol ratios indicated that thermal decomposition was significant only at temperatures above 320°C and would not account for the magnitude of phenyl disulfide conversion observed.

CONCLUSIONS

The principal products arising from the liquid phase oxidation of thiophenol by peroxides formed in situ by reaction of the dodecane with dissolved oxygen at elevated temperatures were identical to those identified in the model studies. Thus, these data indicate that the findings of the model studies can be applicable to aircraft fuel systems. The major route of oxidation of thiophenol most likely involved the donation of a hydrogen radical to the dodecoxy radical. While the resultant alcohol was not detected, interaction with dodecylperoxy radical would result in the formation of dodecyl hydroperoxide. However this is ruled out since hydroperoxides were not detected. While in the model studies, the disproportionation of tBHP was responsible for providing the alkoxy radicals, in the JFTOT, dodecane autoxidation provided the source of free radicals. Due to the ease of formation of the thiylphenyl radical, free radical chains were effectively terminated thus suppressing formation of dodecyl hydroperoxide. Although oxidation of thiophenol by dissolved oxygen in the JFTOT was not significant, thermal decomposition of thiophenol was observed to occur above 280°C to form the disulfide.

The behavior of hexyl disulfide in the JFTOT was consistent with an oxidation mechanism which involves coordination of oxygen to the sulfur centers. Since disulfides cannot act as peroxide reducers, by donating hydrogen radicals, minimal effects were realized on peroxidation during short reaction times in the JFTOT. There was no evidence of direct oxidation of the disulfide by dissolved oxygen.

LITERATURE CITED

1. Hazlett, R. N. and Hall, J. M., 1985. "Jet Aircraft Fuel System Deposits in Chemistry of Engine Combustion Deposits". L. B. Ebert, ed., Plenum Press: New York, 245-261.

2. Scott, G., 1965. "Atmospheric Oxidation and Antioxidants". Elsevier: Amsterdam, Chapter 3.

3. Nixon, A. C., 1962. "Autoxidation and Antioxidants of Petroleum, in Autoxidation and Antioxidants". Lundberg, W. O. ed., Wiley Interscience: New York, 695-856.

4. ASTM "Standard Specification for Aviation Turbine Fuels". In Annual Book of ASTM Standards; ASTM: Philadelphia, 1987; Part 23, ASTM D1655-82.

5. Taylor, W. F., 1976. "Deposit Formation From Deoxygenated Hydrocarbons II. Effects of Trace Sulfur Compounds". Ind. Eng. Chem. Prod. Res. Dev., 15, 64-68.

6. Coordinating Research Council, 1979. "CRC Literature Survey on the Thermal Oxidation Stability of Jet Fuel". CRC Report No. 509; CRC, Inc: Atlanta, GA.

7. Taylor, W. F., and Wallace, T. J., 1968. "Kinetics of Deposit Formation from Hydrocarbons". Ind. Eng. Chem. Prod. Res. Dev., 7, 198-202.

8. Taylor, W. F., and Frankenfeld, J. W., December 1975. "Development of High Stability Fuel". Final Report for Phase II, Contract Nol N00140-74-C-0618, Exxon/GRU.15GAF.75.

9. Wallace, T. J., 1964. "Chemistry of Fuel Instability". In Advances in Petroleum Chemistry and Refining, Wiley-Interscience: New York, 353-407.

10. Daniel, S. R. and Heneman, F. C., 1983. "Deposit Formation in Liquid Fuels: Effects of Selected Organo-Sulphur Compounds on the Stability of Jet A Fuel". Fuel, 62, 1265-1268.

11. Mushrush, G. W. and Hazlett, R. N., 1985a. "Liquid Phase Radical Reactions of Octanal and tert-Butyl Hydroperoxide." J. Org. Chem., 50, 2387-2390.

12. Mushrush, G. W., Hazlett, R. N. and Eaton, H. G., 1985b. "Liquid Phase Oxidation of Undecanal by t-Butylhydroperoxide in Dodecane." Ind. Eng. Chem. Prod. Res. Dev., 24, 290-293.

13. Mushrush, G. W., Watkins, J. M., Hazlett, R. N. and Hardy, D. R., 1987. "Liquid Phase Oxidation of Hexyl Sulfide and Dodecanethiol by t-Butyl Hydroperoxide in Benzene and Tetradecane". Ind. Eng. Chem. Prod. Res. Dev., 26, 662-667.

14. Watkins, J. M., Mushrush, G. W. , Hazlett, R. N. and Beal, E. J., 1988. "Hydroperoxide Formation and Reactivity in Jet Fuels". Energy & Fuels, accepted for publication.

15. Hazlett, R. N., Hall, J. M. and Matson, M., "Reactions of Aerated n-Dodecane Liquid Flowing over Heated Metal Tubes", Ind. Eng. Chem., Prod. Res. Dev., (16), No.2, p.171, 1977.

16. Morris, R. E., Hazlett, R. N. and McIlvaine, C. L., 1988. "The Effects of Stabilizer Additives on the Thermal Stability of Jet Fuel". Ind. Eng. Chem. Res., 27, 1524-1528.

17. Oae, S. (Ed.), "Organic Chemistry of Sulfur". Plenum Press, New York, 1977.

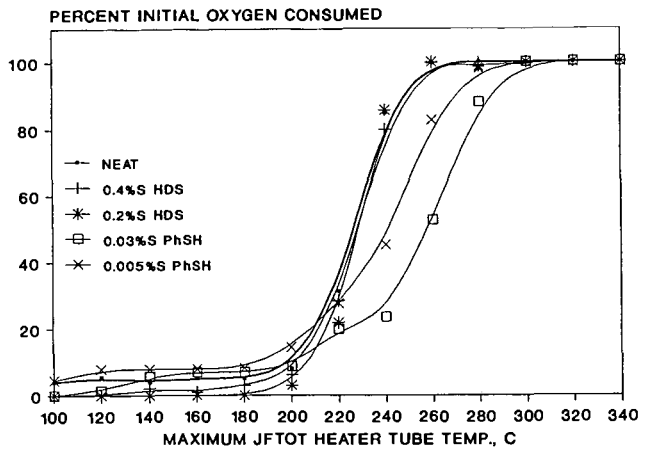

Figure 1. Temperature Dependence of Oxygen Consumption by neat and Doped Dodecane During Stress in the JFTOT.

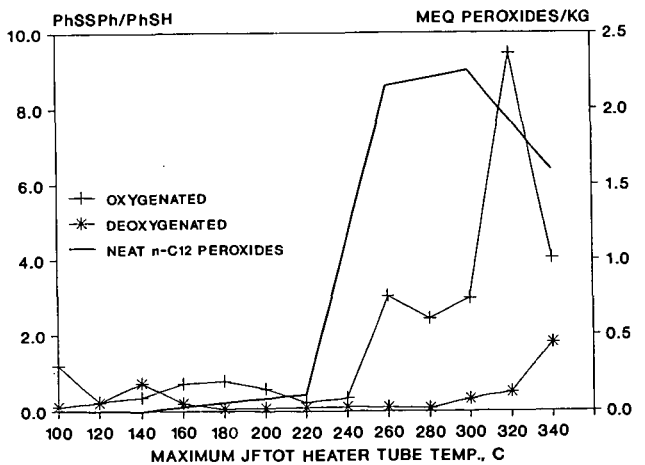

Figure 2. Phenyl Disulfide/Thiophenol Conversion Ratios by GC/MS (left ordinate scale) and Peroxidation of Neat Dodecane (right ordinate scale).

ESCA AND FTIR STUDIES OF BITUMINOUS COAL

Cara L. Weitzsacker, James J. Schmidt
Joseph A. Gardella, Jr.

Department of Chemistry and Surface Science Center
University of Buffalo, SUNY, Buffalo, NY 14214

ABSTRACT

Bituminous coal from the Illinois #6, Upper Freeport, Pittsburgh and Kentucky #9 seams were examined by Electron Spectroscopy for Chemical Analysis (ESCA) and Fourier Transform Infrared Spectroscopy (FTIR). These coals were stored under various conditions (air, N_2, mine water) and received in forms progressing from raw to ash - removed coal, (raw, milled, processed). ESCA was utilized to determine surface elemental composition and functional groups with particular attention given to C,O,N and S. Sulfur and oxidized coal models have been examined to determine the sulfur and carbon species present at the surface. FTIR has been used to correlate functional group assignments with the ESCA results.

INTRODUCTION

The surface composition characteristics of coal are important to the behavior of coal in various processing techniques. This study focuses on the surface of coal in powder form, with emphasis on the elemental composition of the surface of coal, and the functionality of C, O, N and S. One interesting application of this information would be to study the wettability of coal, of concern in agglomeration in various cleaning processes. Agglomerated coal could be separated from mineral matter.(1,2)

Both ESCA and FTIR were used in the study of four bituminous coals. These coals were taken from the Illinois #6, Kentucky #9, Pittsburgh and Upper Freeport seams. The ROM coals were stored under three conditions - in ambient air, mine site tap water and dry nitrogen. Portions of these samples were also milled and processed (mineral matter removed), and these were then analyzed. These samples will serve as reference samples for an ongoing aging experiment to be described in later papers.

EXPERIMENTAL

Raw, milled and processed coals were received under N_2 in sealed bottles from Otisca Industries, Ltd. Raw coals were analyzed as received. Milled and processed coals had to be vacuum dried to remove water and water/pentane respectively. All samples were stored under dry N_2 when received.

Vacuum drying was done on a glass vacuum line. Samples were manipulated under dry N_2 when loaded in vacuum tubes and when the dried coal was removed from the vacuum tube. A liquid nitrogen trap was used to prevent pump oil from backstreaming onto the samples. Samples were evacuated at room temperature for five hours. After vacuum drying all three types of samples were treated the same for sample preparations. Air exposure has been minimized to less than two minutes for the transfer of samples into instruments.

ESCA spectra were recorded on Physical Electronics Model 5100 with a Mg $K_{\alpha 1,2}X$ - ray source (1253.6 eV). Experimental conditions of the X - ray were 300 W, 15 kV and 20 mA. Base pressure of the instrument was 2 x 10 (-9) torr and operating pressure ranged from 1 x 10 (-7) to 2 x 10 (-8) torr depending on the sample. The pass energy was 35 eV for high resolution narrow scans. All spectra were taken using a 45° take - off angle. The sampling depth at this take - off angle was approximately 60 Å.

For ESCA analysis sample preparation was accomplished by pressing coal powder onto double - sided sticky tape on a sample stage. The coal was transferred immediately to the introduction chamber of the instrument and pumped down for one hour before being moved into the main chamber for analysis. Wide scan spectra were taken for 15 - 20 minutes, followed by high resolution narrow region scans for a total of 50 minutes. There was no evidence of sample damage after 65 - 70 minutes under the X - ray.

Infrared spectra were acquired on two different FTIR systems. The first system was a Nicolet 7199A FTIR Spectrometer with an MCT detector. The bench was purged with dry air. Spectra were taken with 1000 scans. The second instrument was a Mattson Alpha Centauri with a DTGS detector. The bench was purged with dry N_2. Spectra acquired were the result of 32 scans.

Samples for FTIR were prepared by KBr mull. Approximately .42g KBr was mixed with .006 - .01g of coal. The mull was pressed into a KBr pellet using a 13mm die under 8000 psi for 45 - 60 seconds.

RESULTS AND DISCUSSION

For this study, seven samples from each of the four seams were analyzed. In each sample set, three samples were raw coal (stored under air, N_2 or water), two were milled (air stored) and two were processed (stored under air and N_2). Tables 1 - 3 show surface atomic concentration results from ESCA analysis. Common to every one of these samples was the detection of C,O, and N. Sulfur was not detectable on the surface of three of the raw samples. Other elements found were Al, Si, Na, Fe and K. Na was found in both the Illinois #6 and Upper Freeport coals. Fe and K were only found in one of the Illinois raw samples.

Inorganic elements were detected in the greatest quantities in the raw samples. The percent surface atomic

concentrations decreased slightly after milling and decreased significantly after the coal was processed. In the processed samples, the inorganics were reduced to less than 1 % or, in many cases, were no longer detectable.

The storage conditions of the raw coals only showed a significant difference in the Illinois #6 and Upper Freeport coals. In the Kentucky #9 and Pittsburgh coals, the resultant % surface atomic concentrations were consistent through all three storage conditions. See Table 1. The two milled samples of Illinois #6 also showed inconsistency in the % surface atomic concentrations. For the other three coals, % surface atomic concentrations of the two milled samples were approximately equal. See Table 2. In the processed coals, the % surface atomic concentration of carbon was 85 - 88 % through all four coals. The % surface atomic concentration of oxygen was 10 - 12 %. Nitrogen remained consistent through all storage and processing steps, with a % surface atomic concentration of approximately 1 - 2 %. The % S remaining in the processed coals varied from .50 - 1.1 %. See Table 3.

In ESCA analysis, differential charging of the inorganic and organic species in the coals was noted. Standards consisting of mineral matter from each mine were run to determine the charge correcting for the inorganics. Si, Al, Na, K, Fe and inorganic S were corrected using Si (SiO_2), binding energy 103.4 eV. The organic species (C, O, N and organic S) were charge corrected using C 1s (hydrocarbon), binding energy 285.0 eV.

The C 1s region was curve fitted to five bands (3,4). See Table 4 and Figure 1. The initial band was set after standards of graphite were analyzed. This peak was at a binding energy of 284.6 eV. Oxidized coal was also analyzed to solidify the assignments of the carbon / oxygen species. Quantitation was done based on the curve fits. See Table 5. From raw to processed coal, a decrease is seen in the elemental / graphitic C and an increase in the aliphatic / aromatic C. C - O remained consistent, while C = O varied widely.

Sulfur has also been found to be present in inorganic and organic species. The inorganic sulfur is postulated to be sulfate compounds. In many samples, nitrogen appears as a broad peak at approximately 400 eV. Pyridine and pyrrole (5) appear at approximately 398.8 and 400.2 eV. It is postulated that both of these could be present.

Transmission FTIR spectra of all samples were collected. Correlations between FTIR and ESCA results support the observations of changing surface composition as raw coals went through processing. Peaks assigned to inorganics such as silicates vary in intensity proportional to the quantities found by ESCA. Similiar correlations are found with the

organics.

CONCLUSIONS

ESCA and FTIR are useful methods in the analysis of coal surfaces. Composition and surface functionality can be elucidated. FTIR can be used to correlate these results deeper into the sample by transmission experiments.

ACKNOWLEDGEMENTS

Support for this work has been provided by the Department of Energy under Contract # DE - AC22 - 87PC79880 DOE Pittsburgh Energy Technology Center with a subcontract to Otisca Industries Ltd.

REFERENCES

1. Schobert, H. H., 'Coal The Energy Source of the Past and Future'; American Chemical Society: Washington DC 1987

2. Frederick Simmons; private communications

3. Perry, D. L. and Grint, A., FUEL 1983, 62, 1024 - 1033

4. Wandass, J. H.; Gardella,Jr., J. A.; Weinberg, N. L.; Bolster, M. E.; Salvati,Jr., L. J. Electochem. Soc. 1987, 134 (11), 2734 - 2739

5. Bartle, K. D.; Perry, D. L.; Wallace, Fuel Process. Technol. 1987, 15, 351 - 361

TABLE 1

	Illinois Raw			Kentucky Raw		
	Air	N	Water	Air	N	Water
C	43	23	33	71	69	71
O	40	51	48	21	22	22
N	1.1	.60	1.1	2.0	1.8	1.0
S	.30	---	---	1.1	1.2	1.2
Al	5.0	7.9	6.5	2.4	2.6	1.2
Si	9.2	15	11	3.2	3.5	2.8
Na	1.4	1.9	1.4	---	---	---
Fe	---	3.1	---	---	---	---
K	---	.89	---	---	---	---

TABLE 2

	Illinois		Pittsburgh	
	Milled			
C	54	66	72	72
O	35	27	22	22
N	1.5	1.5	1.5	1.5
S	.67	.45	.54	.62
Al	3.4	2.2	2.0	2.1
Si	5.9	4.4	3.3	3.5
Na	.50	.86	---	---

TABLE 3

	Illinois		Upper Freeport	
	Processed			
	Air	N	Air	N
C	85	85	86	88
O	12	12	9.7	9.4
N	1.2	1.5	1.8	1.4
S	.72	1.1	.86	.52
Al	---	---	.74	---
Si	.92	.55	1.0	.44
Na	---	---	---	---

TABLE 4

I		284.2 eV	graphitic / elemental C
II	~	285.0 eV	hydrocarbon (aliphatic or aromatic)
III	~	286.6 eV	C - O
IV	~	288.0 eV	C = O
V	~	290.5 eV	COOH, carbonate or π to π^* shakeup

TABLE 5

% C Species by Curve Fitting

Illinois #6

	Raw	Milled	Processed
I	13.85	2.61	2.43
II	58.22	67.27	70.70
III	19.24	17.25	18.26
IV	7.02	9.46	3.88
V	1.67	3.41	4.73

Figure 1

C 1s Region Illinois #6 Milled Coal

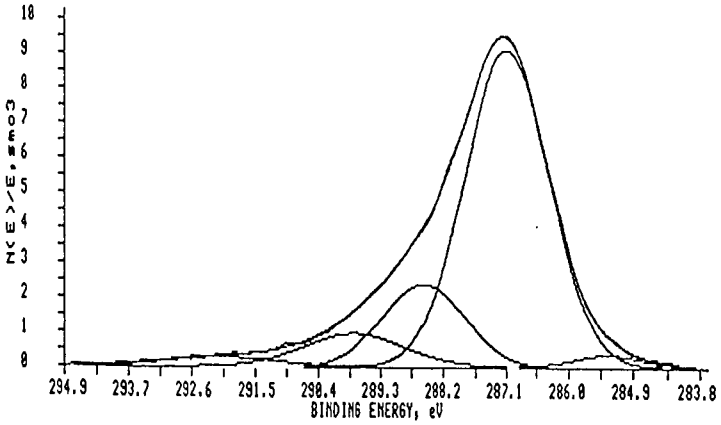

THE FORM-OF-OCCURRENCE OF CHLORINE IN U.S. COALS: AN XAFS INVESTIGATION

Frank E. Huggins[1], *Gerald P. Huffman*[1], *Farrel W. Lytle*[2], *and Robert B. Greegor*[2]

[1]University of Kentucky, Lexington, KY 40506
[2]The Boeing Company, Seattle, WA 98124

ABSTRACT

X-ray absorption fine structure (XAFS) spectroscopy determinations have been made at the chlorine K absorption edge on a number of U.S. coals in order to investigate the form-of-occurrence of chlorine in the coals. The coals vary in chlorine content from 0.04 to 0.84 wt% and in rank from lignite to hvA bituminous. For the most part, the chlorine K-edge XAFS spectra of the coals are very similar and no significant variation is noted among spectra of leached samples of the same coal. The coal XANES spectra differ significantly from spectra of all organo-chlorine compounds and inorganic chlorides examined. However, spectra of hydrated chloride species, including NaCl solutions and $CaCl_2.6H_2O$, and of organic hydro-chlorides, are quite similar to the coal spectra. Analysis of the EXAFS region for the coals suggests the presence of a relatively long bond (~3.0 - 3.1Å) to water molecules in the nearest neighbor shell around the chlorine. These data and results are compatible with hydrated chloride anions in the moisture associated with coals as the major form-of-occurrence of chlorine in U.S. coals.

INTRODUCTION

Coals with appreciable chlorine contents (>0.3 wt%) can be troublesome during utilization due to the corrosive effect of chlorine on both metallic and ceramic materials. In the U.S., such problems related to chlorine content are relatively uncommon except for certain deep-mined coals from the Illinois basin in which the chlorine contents can be as high as 1 wt% (1). Although much of the chlorine in Illinois coals can be removed by aqueous leaching treatments (2,3), the form-of-occurrence in these and other U.S. coals is still not known with any certainty. Float-sink tests for "organic affinity" as developed by Zubovic (4) do not appear to have been applied to chlorine in U.S. coals. Compositional correlations have been used to suggest that chlorine has both inorganic (NaCl) and organic forms in Illinois coals (1,5). Conversely, the lack of the association of chlorine with other elements in a microprobe study of Upper Freeport coal has been interpreted as indicating organic chlorine forms (6). However, other investigators, based largely on microscopic examinations, list only inorganic chlorides, such as NaCl, KCl, $MgCl_2.6H_2O$, etc., as the primary occurrences of chlorine in coal (7,8). Chakrabarti (9), working principally with Gondwana coals, has described detailed analytical procedures for determining both organic and inorganic forms of chlorine in coal. British researchers working with their native high chlorine coals for the most part have proposed that most, if not all, of the chlorine in coal is inorganic and derived from NaCl-rich ground waters penetrating the coal seam (10,11). Recent pyrolysis/mass spectroscopic work (12) on British coals has rather convincingly confirmed this occurrence.

X-ray absorption fine-structure (XAFS) spectroscopy is perhaps the best method currently available for elucidating the local structure and bonding of a specific element in a complex, heterogeneous, noncrystalline matrix such as coal. Not only can the element be investigated directly in coal at quite dilute levels (~100 ppm), but, in principle, information about the immediate coordinating ligands can also be derived from an analysis of the XAFS spectrum. In this work, XAFS spectroscopy

was used to examine the occurrence of chlorine in a number of U.S. coals. From these measurements it can be concluded that much, if not all, of the chlorine in these coals is present as chloride anions in the moisture associated with the pores and microcracks of the coal matrix.

EXPERIMENTAL

Samples: Pulverized samples of as-collected Illinois basin coals and the same coals subjected to an aqueous leaching treatment were provided by Professor H. L. Chen, Southern Illinois University. These samples were originally collected by the Illinois State Geological Survey. Other coal samples used in this study were selected from the Pennsylvania State University coal bank on the basis of their high chlorine contents. Chlorine contents and apparent rank data for the coals are listed in Table I. A large number of standard organochlorine compounds and inorganic chlorides were also assembled for XAFS spectral measurements, including:

Aryl chlorides: 1,2,4,5-tetrachlorobenzene, 9,10-dichloroanthracene, 2,6-dichlorophenol;

Acyl chlorides: diphenylacetyl chloride, 2-naphthoyl chloride;

Alkyl chlorides: polyvinylchloride, 1,2-bis(chloromethyl)benzene, 1,4-bis(chloromethyl)benzene;

Org. hydrochlorides: semicarbazide hydrochloride, tetracycline hydrochloride;

Gases and vapors: Cl_2, CCl_4, $C_2H_4Cl_2$;

Alkali chlorides: NaCl, KCl, RbCl, CsCl, saturated NaCl solution;

Alk. earth chlorides: $CaCl_2$, $SrCl_2$, $CaCl_2.2H_2O$, $CaCl_2.6H_2O$;

Misc. Cl compounds: $KClO_3$, $H_2PtCl_6.6H_2O$, Hg_2Cl_2, $HgCl_2$, $CuCl_2$, $CuOCl$.

XAFS Experiments: XAFS experiments were performed at the Stanford Synchrotron Radiation Laboratory (SSRL) under dedicated running conditions. Electron energies were held at 3.0 Gev while the beam current decayed from 80 to 40 mA between beam fills, which were typically eight hours or more apart. A pure helium path to the sample was employed to minimize attenuation of the X-ray intensity at the low energies in the vicinity of the chlorine K absorption edge (2820-2835 eV). XAFS spectra were recorded in fluorescent geometry in a Stern-Heald type detector (13) for all coals and standards from approximately 100 eV below the edge to about 400 eV above the edge using a rotating double crystal Si(111) monochromator. At the high-energy end of the scan, the K absorption edge for argon (from air contamination in the beam path) was encountered at 3205 eV. This edge served effectively as an internal energy calibration point. The X-ray near-edge structure (XANES) data and spectra shown in the paper are given relative to the zero point defined as the maximum in the differential of the XAFS spectrum of sodium chloride, which occurs at 2826 eV. It was found that the variation in position of the argon edge relative to the NaCl zero point was less than 0.1 ev for the different spectra measured. Spectra were obtained from the coal samples and from solid standards as pressed pellets in pressed boric acid (HBO_3) supports; liquid samples were contained in mylar bags or on filter papers; gaseous and vaporous species were introduced to the sample chamber at dilute (<1%) levels in helium (14). Analysis of the spectral data was performed on a MicroVAX II computer using conventional methods (15,16) for the XANES and extended fine-structure (EXAFS) regions of the spectra.

TABLE I: COALS EXAMINED BY CHLORINE XAFS

Coal Seam & State	Rank	Wt% Chlorine	Source
#6 seam, Illinois*	hvAb	0.82	C-20154 (ISGS)
#6 Seam, Illinois*	hvAb	0.42	C-8601 (ISGS)
-- after 1st. leaching		0.24	
-- after 2nd. leaching		0.12	
#6 Seam, Illinois*	hvAb	0.42	C-22175 (ISGS)
-- after 1st. leaching		0.18	
-- after 2nd. leaching		0.13	
Pittsburgh, PA	hvAb	0.22	USS Mining
Elkhorn #3, KY	hvAb	0.33	PSOC - 1475
Mineral seam, KS	hvAb	0.27	PSOC - 251
Mineral seam, OK	hvAb	0.24	PSOC - 768
Wildcat sbb, TX	sbbC	0.06	PSOC - 639
Beulah lignite, ND	lig	0.04	PSOC - 1483

*supplied by Prof. H. L. Chen, Southern Illinois University

RESULTS

XANES Spectra: Figure 1 shows the XANES spectra of an Illinois #6 coal that contains 0.42 wt% chlorine and two samples obtained from the coal after aqueous leaching treatments (2,3) that first reduced the chlorine content to 0.24 wt% and then to 0.12 wt%. It is obvious from this sequence that the chlorine K-edge absorption spectrum is not significantly changed by the leaching treatments and therefore it can be concluded that chlorine has only one significant form-of-occurrence in this coal. Furthermore, the reason that chlorine becomes progressively more difficult to remove from the coal is not because of the response of different forms of chlorine to the leaching treatment but because the one form-of-occurrence of chlorine becomes less accessible or more strongly bound to the coal as its abundance decreases.

Very similar XANES spectra to those in Figure 1 are exhibited by all the coals listed in Table I with two exceptions: the Illinois coal with the highest chlorine content (0.84 wt%) and the Beulah lignite with the lowest chlorine content (0.04 wt%). Figure 2 documents the similarity of the chlorine K edge XANES spectra of three coals from different coal basins. Figure 3 shows the XANES spectrum of chlorine in the two Illinois coal with highest chlorine contents. The differences between these spectra can be explained readily by the presence of a minor component (<25%) of crystalline NaCl in the Illinois #6 coal with 0.84 wt% chlorine. The extra peaks in the spectra of this coal match exactly with prominent peaks in the spectrum of NaCl, which is also shown in Figure 3. The XANES spectrum of the Beulah lignite, although very weak, differs significantly from those of the other coals and the position of its main peaks are well outside the ranges for the two peaks present in the spectra of the coals of higher rank. Based on XANES peak position

TABLE II: CHLORINE XANES DATA SYSTEMATICS*

Compound	Zero Point (ev)	1st. Peak (ev)	2nd. Peak (ev)
Mercury chlorides	-3.62 - -3.60	-3.0 - -2.6	13.4 - 13.6
Alky' chlorides	-3.35 - -2.80	-2.5 - -1.2	11.0 - 20.8
Acyl chlorides	-2.60 - -2.50	-1.3 - -1.0	15.3 - 20.9
Aryl chlorides	-2.40 - -2.00	-0.8 - -0.4	16.1 - 19.2
Beulah lignite	-1.80	-0.7	18.5
All other coals	-1.75 - -1.20	0.9 - 1.3	19.0 - 21.2
Sat. NaCl solution	-1.55	0.2, 3.1	20.9
Organohydrochlorides	-1.10 - -1.00	1.1 - 2.1	19.2 - 20.7
Alkali chlorides	-0.90 - 0.00	0.4 - 2.2	16.9 - 20.6
Hydrated Ca chlorides	-0.75 - -0.60	2.3 - 2.5	21.6
Alk. earth chlorides	-0.60 - -0.45	1.7 - 2.1	19.0 - 19.6
Copper chlorides	-0.60 - -0.30	1.4 - 3.0	19.8 - 27.3
Chloroplatinic acid	-0.20	4.2	18.7
Potassium chlorate	4.20	5.8	18.5

Energies of zero point and peaks relative to zero point for NaCl.
*For most standard chlorine compounds, data are given only for the two peaks that most closely match the peaks in the coal spectra.

systematics (Table II), the XANES spectrum from chlorine in the lignite is most similar to that from chlorine bound to aromatic rings. However, given the low abundance of chlorine in this coal and the poor quality spectrum, it is perhaps premature to conclude that this coal has a significantly different form-of-occurrence for chlorine.

With the possible exception of the lignite, the data in Table II and the general appearance of the XANES spectra from chlorine in the coals, compared to those of the numerous standard chlorine compounds examined, indicate that the form-of-occurrence of chlorine is clearly neither an organochlorine compound nor one of the traditional crystalline inorganic chlorides. The substances that most closely resemble the XANES spectral data from chlorine in coal are (i) $CaCl_2.6H_2O$, (ii) saturated NaCl solution, and (iii) organohydrochlorides. A comparison of the XANES spectra of these substances to that of the Illinois #6 coal is shown in Figure 4. The XANES spectra of all three substances exhibit an overall general similarity to the coal spectra, but minor dif-ferences are apparent upon close inspection so that it can not be concluded that one or other of these substances is the preferred match. However, all three substances do have some structural and bonding features in common that are, no doubt, reflected in similar XANES spectra: (i) chlorine is present in these substances as chloride anions, (ii) the bonding is relatively weak and largely ionic in character, and (iii) the chlorine-oxygen or chlorine-nitrogen distances are quite long: between 3.0 and 3.2Å (17,18). The chlorine in coals can be expected to be similar.

EXAFS Spectra: As is usually done (15,16), the EXAFS regions of the spectra were treated mathematically first to isolate the EXAFS periodic structure from the absorption step. Then, by converting this oscillatory structure to a wave vector representation and performing a Fourier transform, a radial structure function (RSF)

is obtained that represents the distribution of shells of atoms or ions around the chlorine atom or ion. Satisfactory radial structure functions were obtained for most of the standard compounds and for some of the coals with the higher chlorine contents. RSFs for the aryl compounds were noticeably more complex than those for the acyl and alkyl organochlorine compounds. This observation reflects the rigid structural relationship of the chlorine to the six carbons of the benzene ring present in the aryl compounds but which is lacking when chlorine is in a peripheral -COCl or -CH_2Cl group that has some rotational freedom. The RSFs for compounds with these latter groups resemble those obtained from the simple molecules, CCl_4, $C_2H_4Cl_2$, etc.

Radial structure functions for chlorine in the inorganic compounds were generally complex and lacking in any strong correlative trends. Given the variety of structures and the range in degree of covalency exhibited by these compounds, this should not be surprising. $CaCl_2.6H_2O$ has a structure (17) in which the Ca and Cl ions are not nearest neighbors but are separated by water molecules. Hence, this compound can act as a model compound for chloride anions surrounded by water molecules. The RSF for this compound is shown in Figure 5a; it is dominated by one major peak representing the coordination shell of six water molecules at a distance of 3.1 - 3.2Å from the central chloride anion. Bond-lengths were extracted from the better RSFs of chlorine in coals (e.g. Figure 5b) using the phase-shift data obtained empirically from $CaCl_2.6H_2O$ for the water molecule shell at ~3.15Å. An excellent correlation of the phase shifts was found at a Cl-H_2O distance of 3.03Å for the coals. The phase-shift data correlated considerably better than that between $CaCl_2.6H_2O$ and the saturated NaCl solution, which implies, perhaps, that the chlorine anions in the saturated NaCl solution have significant contribution from sodium ions in the nearest neighbor shell. The RSFs for the organic hydrochloride compounds consist of one major peak at similar distances (3.1 - 3.3Å) arising from nitrogen atoms in basic amine groups to which the chloride anions are bound (18). However, correlation of the Cl-N phase-shift data with the coal data was not as good as that found between $CaCl_2.6H_2O$ and chlorine in coal. Although such distinctions are not necessarily definitive, the analysis of the EXAFS region does appear to favor water molecules as the most likely environment around chlorine in the coals examined.

CONCLUSIONS

Analysis of chlorine K-edge XAFS data for a number of U.S. coals has shown that in the majority of the coals chlorine is present in a single form as chloride anions in the moisture associated with the microcracks and pores of the coal. In the coal with the highest chlorine content, a second form-of-occurrence was also identified, namely crystalline NaCl, which presumably had precipitated from the chloride-rich solution as the coal dried. The only other exception was a low-chlorine lignite, in which chlorine appeared to be present in organic form. However, given the very low chlorine concentration (0.04 wt%) and the related poor spectral quality, it is premature to attach much significance to this observation at this time.

With chloride anions in moisture as the predominant form-of-occurrence of chlorine in U.S. coals, it is relatively easy to rationalize some of the apparently contradictory conclusions made in previous investigations regarding whether chlorine is inorganically or organically bound in coal. As a result of the association of chlorine with coal moisture, chlorine will have properties similar to a dispersed organically bound element. For example, in microprobe or SEM X-ray mapping techniques, chlorine will be found to be distributed widely in low concentrations in macerals and not strongly correlated with other elements, and in float-sink tests of "organic" affinity, chlorine will favor the maceral-rich float fractions.

Conversely, observations of specific inorganic chlorides in coals can be explained as precipitates that crystallize as the coal moisture evaporates.

With the form-of-occurrence of chlorine now established for U.S. coals, it would appear that it should be possible to remove virtually all of the chlorine from troublesome coals by the combination of fine grinding and aqueous leaching treatments. It is interesting to note that a similar treatment was used by British researchers to remove the supposed "organic" chlorine fraction from an Illinois #6 coal that was left after earlier leaching treatments (12). Alternatively, the fact that the chlorine is now known to be associated with the moisture in coal may lead to new methods for chlorine removal.

ACKNOWLEDGEMENTS

We are grateful to Professor Han Lin Chen of Southern Illinois University for providing us with samples of raw and leached Illinois #6 coals. This work was supported by the U.S. DOE under Contract No. DE-FG22-86 PC90520. We also acknowledge the U.S. DOE for its support of the Stanford Synchrotron Radiation Laboratory, where the XAFS experiments were performed.

LITERATURE CITED

1. H. J. Gluskoter, and R. R. Ruch, Fuel, 50, 65, (1971)
2. H. L. Chen, N. M. Rao, and D. S. Viswanath, Fuel Proc. Technol., 13, 261, (1986)
3. H. L. Chen, and M. Pagano, Fuel Proc. Technol., 13, 271, (1986)
4. P. Zubovic in: Coal Science, (ed. R. F. Gould), Advances in Chemistry Series, Volume 55, 221, American Chemical Society, Washington, D. C., (1966)
5. H. J. Gluskoter, R. R. Ruch, W. G. Miller, R. A. Cahill, G. B. Dreher, and J. K. Kuhn, Illinois State Geological Survey, Circular 499, (1977)
6. J. A. Minkin, E. C. T. Chao, and C. L. Thompson, ACS Division of Fuel Chemistry, Preprints, 24(1), 242, (1979)
7. M. T. Mackowsky, Chapter 2.23 in: Stach's Handbook of Coal Petrology, (eds. E. Stach et al.), 121, Gebrüder Borntraeger, Berlin, W. Germany, (1975)
8. R. B. Finkelman, and R. W. Stanton, Fuel, 57, 763, (1978)
9. J. N. Chakrabarti, Chapter 10 in: Analytical Methods for Coal and Coal Products, (ed. C. Karr, Jr.), Vol. 1, 323, Academic Press, New York, (1978)
10. S. A. Caswell, Fuel, 60, 1164, (1981)
11. N. J. Hodges, W. R. Ladner, and T. G. Martin, J. Inst. Energy, 56, 158, (1983)
12. G. Fynes, A. A. Herod, N. J. Hodges, B. J. Stokes, and W. R. Ladner, Fuel, 67, 822, (1988)
13. E. A. Stern, and S. Heald, Rev. Sci. Instrum., 50, 1579, (1979)
14. F. W. Lytle, R. B. Greegor, E. C. Marques, D. R. Sandstrom, G. P. Huffman, and F. E. Huggins, Stanford Synchrotron Radiation Laboratory Activity Report for 1986, 87/01, 115, (1987)
15. P. A. Lee, P. H. Citrin, P. Eisenberger, and B. M. Kincaid, Rev. Mod. Phys., 53, 769, (1981)
16. G. S. Brown, and S. Doniach in: Synchrotron Radiation Research, (eds. H. Winick and S. Doniach), 353, Plenum Press, New York, (1980)
17. R. W. G. Wyckoff, Crystal Structures, Vol. 3, J. Wiley & Sons, New York, (1963)
18. R. W. G. Wyckoff, Crystal Structures, Vol. 6, J. Wiley & Sons, New York, (1969)

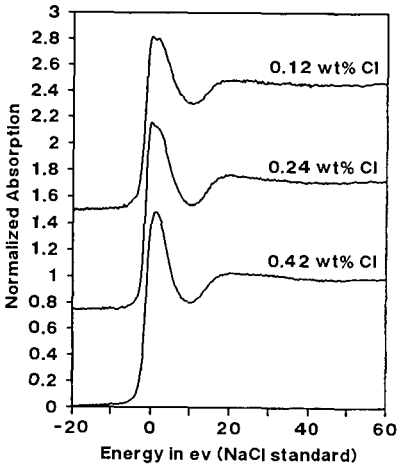

Figure 1. Chlorine K-edge XANES spectra of Illinois #6 coal and two samples of same coal after leaching treatments. Note the similarity of the spectra.

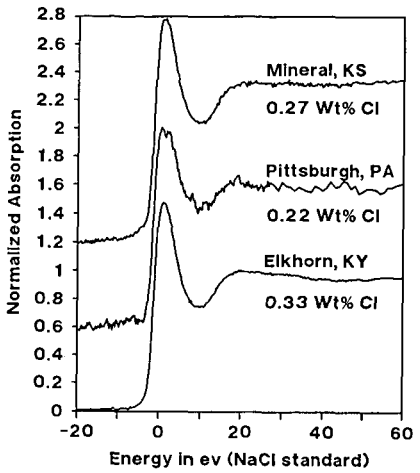

Figure 2. Chlorine K-edge XANES spectra of three coals from different states and geological provenances. Note the similarity of the spectra.

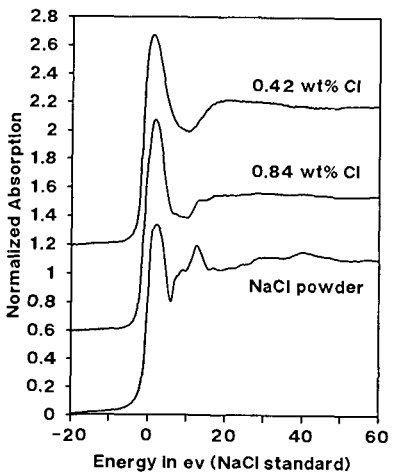

Figure 3. Chlorine K-edge XANES spectra of two high-chlorine Illinois #6 coals and of NaCl.

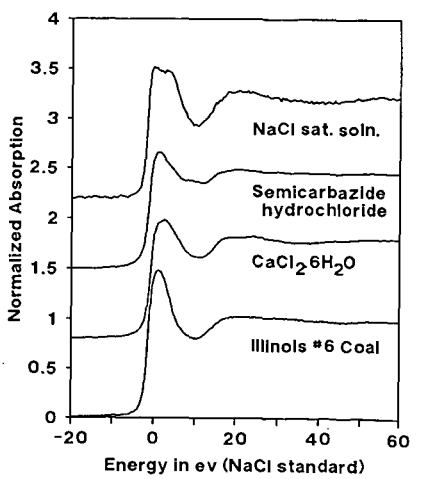

Figure 4. Chlorine K-edge XANES spectra of Illinois #6 coal and various standard Cl compounds with similar spectra.

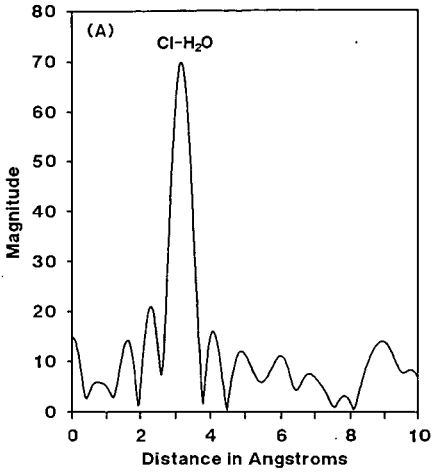

Figure 5(a). Phase-shift corrected radial structure function for the compound, $CaCl_2.6H_2O$.

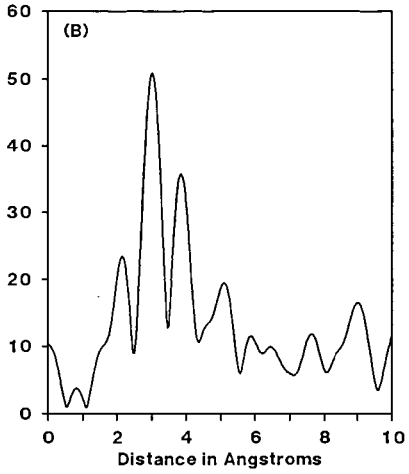

Figure 5(b). Phase-shift corrected radial structure function for chlorine in an Illinois #6 coal.

HYDROGEN BONDING AND COAL SOLUBILITY AND SWELLING

Paul Painter, Yung Park and Michael Coleman

Materials Science and Engineering Department
Steidle Building
The Pennsylvania State University
University Park, PA 16802

Most descriptions of the thermodynamic properties of coal solutions and the swelling of coal are based on models that in their original form only dealt with simple van der Waals or London dispersion forces. It is now well-known that such descriptions are inadequate when applied to systems where there are strong specific interactions such as hydrogen bonds. In part, this is because for weak forces random contacts between unlike segments can be assumed, allowing interactions to be formulated in a mean field form, $\Delta E_{int}\phi_A\phi_B$, where ΔE_{int} is an exchange interaction term; $\phi_A\phi_B$ are the volume fractions of the components A and B and their product is proportional to the number of unlike contacts in a solution where there is random mixing. Hydrogen bonds are different and cannot be dealt with by means of a simple approximation. Polymer segments and solvent molecules that interact in this manner are truly associated and above the T_g there is a dynamic equilibrium distribution of hydrogen bonded species. There is a non-random arrangement of the hydrogen bonding functional groups (relative to one another) and this leads to modifications in the entropy of mixing. Theories that deal only with the enthalpy of hydrogen bonding interactions are thus inadequate.

In recent work (1-4) we have developed an association model that essentially consist of a Flory-Huggins type of equation with an additional term (ΔG_H) describing the free energy changes associated with the changing pattern of hydrogen bonding that occurs as a function of composition:

$$\frac{\Delta G_M}{RT} = \frac{\phi_A}{N_A} \ln \phi_A + \frac{\phi_B}{N_B} \ln \phi_B + \phi_A\phi_B\chi + \frac{\Delta G_H}{RT}$$

Although it may appear that we have arbitrarily added a term accounting for non-random contacts to a random mixing theory, association models are more subtle than that and it can be shown that the above equation can be derived directly from a lattice model (2). The ΔG_H term has a complex appearance (but once you get used to it has an easily understandable structure), but it is important to note that all terms in this equation are determined from experimental FTIR measurements and the equations describing the stoichiometry of hydrogen bond formation. (Space does not permit a reproduction of these equations here, and the interested reader should consult the literature.) Accordingly, given a knowledge of χ, or a reasonable way of estimating this parameter, we could predict the free energy of mixing coal with hydrogen bonding solvents. It is relatively easy to show that the ΔG_H term is either zero or negative, the χ term is positive for purely van der Waals or London dispersion interactions, while the combinatorial entropy term of course favours mixing. The χ and ΔG_H terms have very different temperature dependencies and the balance between these forces leads to the prediction of a rich variety of phase behaviors (2, 4, 5-7). In initial work on coal solutions we have determined general trends, through a calculation of the free energy of mixing pyridine with model coal structures (4).

These initial results provide some fundamental insight, but there now remains the more difficult task of calculating the behavior of specific systems and determine expressions for the chemical potentials, so that the model can be extended to swelling and molecular weight

measurements. Here we consider the first part of this task and we will commence by first defining an average coal structure per OH group. This sounds as if we are arbitrarily classifying a coal molecule as a set of "average" repeat units. In a certain sense we are, but this is not a fallacious approach, as we will show. In the classic work of Scott (8), performed more than thirty years ago, it was demonstrated that the "physical" (ie. non-hydrogen bonded) interactions of a copolymer of any degree of heterogeneity could be described by a solubility parameter that is a volume fraction average of the contributions of its constituents. We can therefore use the method of van Krevelen (9) to determine the parameter δ_{coal}. This requires first of all a knowledge of the coal composition and the relative proportions of aromatic and aliphatic carbon, which have been determined directly for many coals by ^{13}C nmr, or can be estimated from FTIR measurements of the relative proportions of aromatic and aliphatic CH groups. In addition, we also need to define a reference volume for the coal that can correspond to any arbitrarily defined segment (because we will simply calculate the free energy change per segment upon mixing). Van Krevelen (9) calculated his solubility parameter in terms of the molar volume of a coal "molecule" per carbon atom, V_m/C, using:

$$\frac{V_M}{C} = \frac{1200}{C'd}$$

where C' is the weight percent carbon in the sample and d is the density. In the same fashion we define a molar volume per OH group as:

$$\frac{V_M}{O_{OH}} = \frac{1600}{O^1_{OH}d}$$

where O^1_{OH} is the weight percent oxygen in the sample that is present as OH groups (O^1_{OH} and d are known or measurable quantities). This allows us to calculate the free energy contribution from hydrogen bonding interactions per molar volume of the average coal segment containing one OH group.

The χ parameter is then calculated from solubility parameters in the usual fashion, while ΔG_H, the free energy of hydrogen bonding interactions, can be calculated in a straightforward manner by methods we will describe below. The definition of a "segment" of a coal molecular per OH group, therefore merely serves to place the calculations of χ and ΔG_H on a common scale of unit volume. As long as the OH groups in coal are more or less randomly distributed our definition of an arbitrary segment is conceptually sound.

The quantity ΔG_H is calculated from a knowledge of the number of OH groups present in a sample (more precisely, the molar volume per OH group) and equilibrium constants describing the free energy change per hydrogen bond (the equation describing ΔG_H is then a simple counting of the change in the number of hydrogen bonds of various types upon mixing). These are determined by FTIR. Fortunately, we do not have to measure these directly on coal. It is a consequence of the lattice model (2) that equilibrium constants for a particular functional group determined in one molecule can be transferred to a different molecule with the same functional group by simply adjusting according to the molar volume

$$\text{ie. } K^1_B V^1_B = K^2_B V^2_B$$

Using values determined for phenol and cresols ($K^1_B V^1_B$) we can thus calculate appropriate values for a coal segment defined by V^2_B. (This result has worked extremely well in predicting the phase behavior of blends of polyvinyl phenol with various polyethers and polyesters (6). The values of the equilibrium constants describing the self-association of phenol have been determined by Whetsel and Lady (10). (This splendid paper, published in Spectrometry of Fuels a number of years ago, anticipates our use of association models for coal and has the almost forgotten virtue of tabulating all data obtained, in this case in both the near and mid IR. We were thus able to check all calculations and determine the appropriate values of the equilibrium constants.) We have expanded our treatment of self association to

also account for the hydrogen bonds that can form intramolecularly between coal OH and ether oxygens. This is conceptually straightforward and comes at the expense of a minor increase in the algebraic complexity of the equations. The equilibrium constants describing interactions between phenolic OH groups and ethers, and indeed between OH and most of the functional groups found in solvents commonly used to swell coals, are tabulated in the literature (eg see the review by Murthy and Rao (11)). We are fortunate that interactions involving both alkyl and phenolic OH groups have been so widely studied. The parameters used in the calculations are listed in table 1 and our computational procedures are described elsewhere (2-4, 6).

Typical results are shown in figure 1. The data points represent spinodals and were calculated for various coal-pyridine mixtures. This naturally requires that the structural parameters of the coals have been determined and we used a data set compiled for a set of vitrinite concentrates (12). In the accessible range of temperature (up to about the boiling point of pyridine) we determine a classic inverted U shape coexistence curve characterized by an upper critical solution temperature near 0°C, for a coal of 78.3% carbon content. As the carbon content of coal increases the calculated solubility parameter decreases to a minimum near a carbon content of 88% C (9).

For the three coals from which we have performed detailed calculations, with carbon contents of 78.3%, 84.7% and 90.1%, the value of χ thus decreases with increasing carbon content, favoring mixing. At the same time, however, the number of OH groups systematically decreases, thus decreasing the favorable contribution of hydrogen bonding. This latter effect dominates, so as the carbon content of the coal increases we predict that the upper critical solution temperature shifts to higher temperature and for a coal of 90.1% carbon content we calculate spinodals characteristic of a phase separated system throughout the accessible temperature range.

At first sight these results might seem inconsistent with some of the known characteristics of coal (13-18), where swelling reaches a maximum in about the middle range of carbon contents we have considered. It should be kept in mind, however, that in our calculations we have assumed that the chains are not cross-linked (The phase diagrams in figure 1 were determined for a coal molecule of "degree of polymerization" 100, relative to the molar volume of a pyridine molecule). Such molecules are predicted to be soluble at room temperature for a low carbon content coal, and to phase separate into a dilute coal solution and a solvent swollen coal gel at higher carbon contents. The degree of swelling depends not only on the phase behavior of these systems as defined by their chemical potentials, but also upon the degree of cross-linking. We have obtained appropriate expressions for the contribution of hydrogen bonding interactions to the chemical potentials and plan to incorporate these into theories of swelling. Of more interest to us here, however, is the overall effect of hydrogen bonding interactions on phase behavior. Pyridine forms relatively strong bonds with phenolic OH groups, so we would like predict that for solvents that hydrogen bond less strongly, such as THF, the contribution of ΔG_H would be smaller. It must be kept in mind that hydrogen bonding alone does not determine phase behavior, the contribution of the "physical" (usually repulsive) forces measured by χ, together with the combinatorial entropy of mixing, all contribute to the balance. As it happens, the χ value for the coal-THF mixtures considered here are larger than their coalpyridine counterparts and this combined with the smaller contributions to ΔG_H from hydrogen bonding results in the spinodals shown in figure 2, which indicate that the coals are less soluble and would swell less in this solvent.

Obviously solubility is molecular weight dependent and the phase behavior of the 84.7% coal as a function of molecular weight (defined in terms of a degree of polymerization N_B relative to the molar volume of the solvent molecule) is shown in figure 3. This model predicts that for this coal fairly large molecules. ($N_B > 30$) would be soluble in boiling pyridine, although some of the high molecular weight material would

precipitate out at room temperature, depending upon the concentration of the solvent. Only relatively low molecular weight material would be completely soluble in THF.

Finally, we must re-emphasize that for any specific coal the overall phase behavior is determined by the balance between hydrogen bonding and physical forces. The former is measured by the equilibrium constant for association, which we define by the symbol K_A. Values listed in the literature (11) are reproduced in Table 2, together with values of the solubility parameter. For the coals considered here we would therefore qualitatively expect that NMP and pyridine would be the best solvents (large K_A, δ_s in the range 10.7 to 11.5); dimethyl formamide hydrogen bonds strongly but has a somewhat larger χ than these solvents; DMSO hydrogen bonds very strongly but would have an even larger value of χ; while the remaining solvents would not give comparable swelling or solubility characteristics. Obviously detailed calculations are required for quantitative predictions and these are presently being performed.

Acknowledgment. We gratefully acknowledge the support of the Office of Basic Energy Sciences, Division of Chemical Sciences, Department of Energy, under Grant No. DE-FG02-86ER13537.

References

1. Painter, P.C., Park, Y., Coleman, M.M., Macromolecules, 1988, 21, 66.
2. Painter, P.C., Park, Y., and Coleman, M.M., Macromolecules (accepted for publication).
3. Painter, P.C., Park, Y., and Coleman, M.M., Macromolecules (accepted for publication).
4. Painter, P.C., Park, Y., and Coleman, M.M., Energy and Fuels, 1988, 2, 693.
5. Coleman, M.M., Skrovanek, D.J., Hu, J. and Painter, P.C., Macromolecules, 1988, 21, 59.
6. Coleman, M.M., Lichkus, A.M., and Painter, P.C., Macromolecules (accepted for publication).
7. Coleman, M.M., Hu, J., Park, Y. and Painter, P.C., Polymer, 1988,m 29, 1659.
8. Scott, R.L., J. Polym. Sci., 1952, 9, 423.
9. van Krevelen, D.W., Fuel, 1965, 45, 229.
10. Whetsel, K.B. and Lady, J.H. in Spectrometry of Fuels, Friedel, H., ed., Plenum, London, 1970, p. 259.
11. Murthy, A.S.N. and Rao, C.N.R., Applied Spect. Revs., 1968, 2, 69.
12. Painter, P.C. Starsinic, M. and Coleman, M.M. in "Fourier Transform Infrared Spectroscopy", (J.R. Ferraro and L.J. Basile editors) Academic Press (1985), Chapter 5.
13. Green, T., Kovac, J., Brenner, D., Larsen, J.W. in "Coal Structure", Meyers, R.A., ed., Academic Press, New York, 1982.
14. Larsen, J.W. in "Chemistry and Physics of Coal Utilization", AIP Conference Proceedings, No. 70, Cooper, B.R., Petrakis, L., eds., AIP, New York, 1981.
15. Larsen, J.W., Green, T.K. and Kovac, J.J. Org. Chem., 1985, 50, 4729.
16. Lucht, L.M. and Peppas, N.A. in "Chemistry and Physics of Coal Utilization", AIP Conference Proceedings, 18, Cooper, B.R., Petrakis, L., eds., AIP, New York, 1981.
17. Lucht, L.M. and Peppas, N.A., Fuel, 1987, 66, 803.
18. Lucht, J. and Peppas, N.A., J. Appl. Polym. Sci., 1987, 33, 2777.

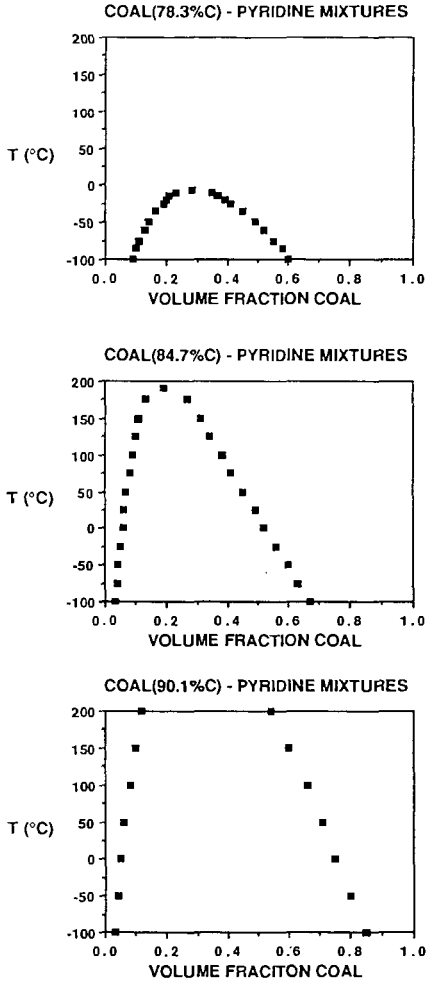

FIGURE 1. Phase diagrams (spinodals) for various coals with pyridine.

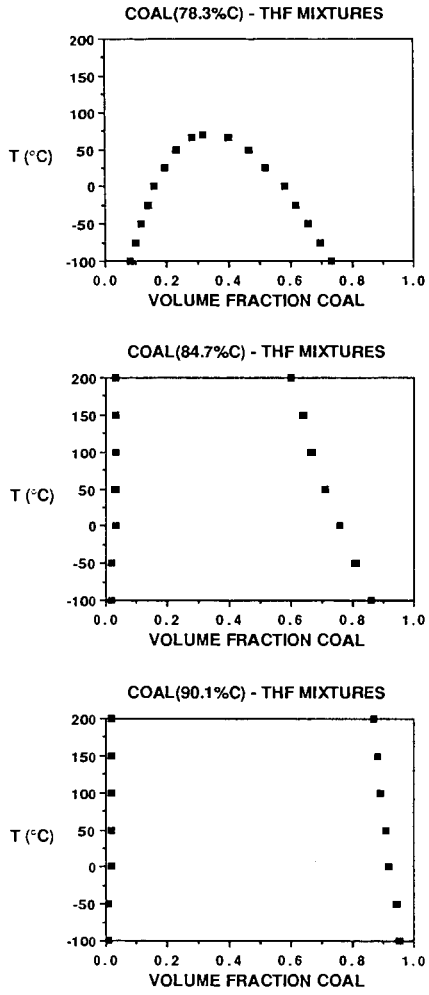

FIGURE 2. Phase diagrams (spinodals) for various coals with THF.

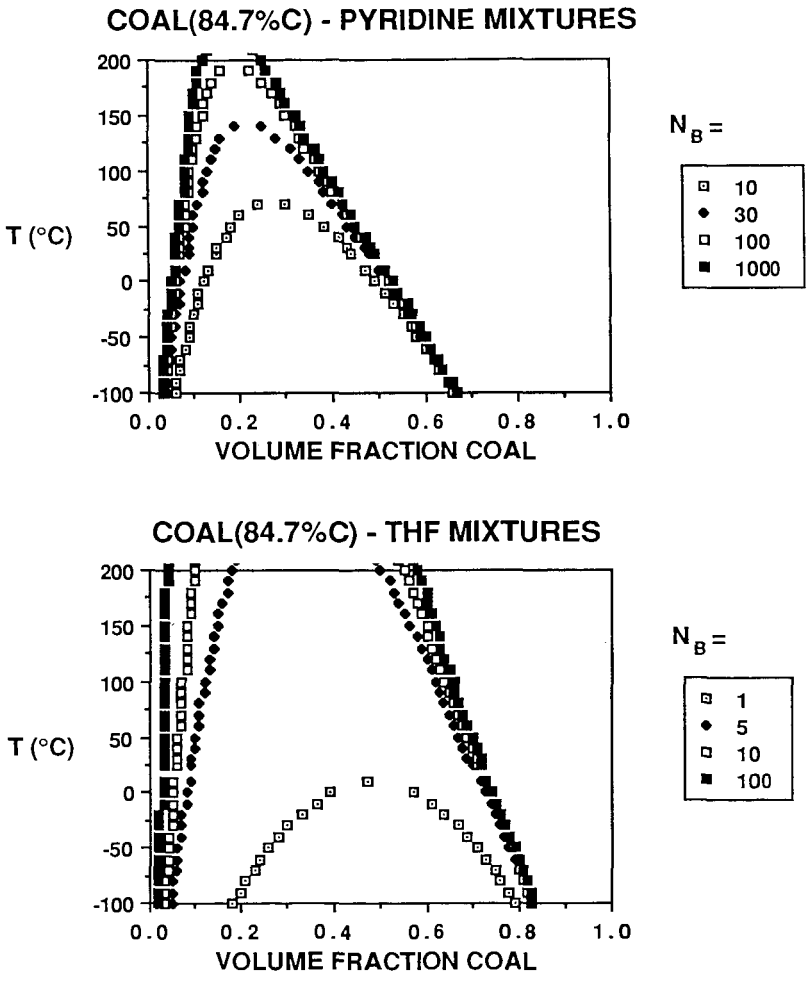

FIGURE 3. Phase diagrams (spinodals) as a function of molecular weight.

Table 1. Parameters for Coal at 25°C

	78.3%C	84.7%C	90.1%C
molar vol, (V_B) $cm^3\ mol^{-1}$	227.92	286.23	4102
molar vol, (V_E) $cm^3\ mol^{-1}$	151.95	384.62	440
δ_C, $(cal\ cm^{-3})^{1/2}$	11.5	11.27	10.78
K_2	8.33	6.64	0.46
h_2, kcal mol^{-1}	5.6	5.6	5.6
K_E	19.44	15.48	1.08
h_E, kcal mol^{-1}	5	5	5
K_B	26.67	21.23	1.48
h_B, kcal mol^{-1}	5.2	5.2	5.2

Parameters for Solvents at 25°C

	pyridine	THF
molar vol, (V_S) $cm^3\ mol^{-1}$	81	74.3
δ_S, $(cal\ cm^{-3})^{1/2}$	10.6	9.9

Table 2

SOLVENT	K_A (l mol^{-1}) (20°C)	δ_S ($cal\ cm^{-3}$)
PYRIDINE	60	10.6
NMP	163	11.2
DIMETHYL FORMAMIDE	64	12.1
DMSO	60	10.6
THF	18.8	9.9
ACETON	12.3	9.9
DIETHYL ETHER	9.6	7.5
ACETONITRILE	5.0	11.8
BENZENE	0.3*	9.1

* Weak H-bonds between OH groups and Π electrons have been proposed.

REGIOSELECTIVE THERMOLYSIS OF 1,4-DIPHENYLBUTANE ENHANCED BY RESTRICTED RADICAL MOBILITY

P. F. Britt, A. C. Buchanan, III, and C. A. Biggs
Chemistry Division
Oak Ridge National Laboratory
P. O. Box 2008
Oak Ridge, TN 37831-6197

INTRODUCTION

Thermal decomposition of coal has been postulated to involve the formation of free radicals by processes such as the homolysis of aliphatic or ether-containing bridges which connect polycyclic aromatic units into a macromolecular structure.[1] Understanding the thermal reactivity of coal is important in the study of pyrolysis, liquefaction, and coking.[2] Mechanistic insights into the chemical reactivity of coal at the molecular level can be gained from the study of model compounds which represent structural features in coal. However, radicals generated in a cross-linked macromolecular material such as coal may experience restricted mobility when the radical center remains bound to the residual molecular structure. To model the effects of restricted radical mobility on thermally induced decomposition reactions, thermolyses of model compounds covalently attached to an inert support have been studied. Thermolysis of surface-immobilized 1,2-diphenylethane showed a substantially altered free radical reaction pathway compared with the corresponding liquid phase behavior,[3] while thermolysis of surface-immobilized 1,3-diphenylpropane (~~DPP) showed unexpected regioselectivity resulting from conformational restrictions on hydrogen transfer reactions as the surface coverage of ~~DPP decreased.[4] In order to further explore the regioselectivity of hydrogen transfer induced by restricted diffusion, the thermolysis of surface-immobilized 1,4-diphenylbutane (~~DPB) is being examined.

EXPERIMENTAL

p-(4-phenylbutyl)phenol (HODPB) was prepared in a four-step synthesis from the Wittig reaction of cinnamyltriphenylphosphonium chloride with *p*-anisaldehyde to afford 1-(4-methoxyphenyl)-4-phenyl-1,3-butadiene which was catalytically reduced (10% Pd/C) and demethylated (HBr/HOAc). Repeated crystallizations from hexanes afforded HODPB in >99.9% purity (GC). Surface-immobilized 1,4-diphenylbutane was prepared at saturation coverage by condensation of excess HODPB with the surface hydroxyls of a high purity fumed silica (Cab-O-Sil, M-5, Cabot Corp., 200 m^2/g) at 225°C for 1 h, as previously described.[3] Excess phenol was sublimed from the Cab-O-Sil by heating at 270°C for 45 min under vacuum (5×10^{-3} Torr). Following base hydrolysis of the Cab-O-Sil (to liberate surface-bound phenol) and silylation, GC analysis gave coverages for three different batches as 0.504, 0.548, and 0.541 mmol of ~~DPB per gram of final product with a purity >99.7%.

Thermolysis of ~~DPB was performed at 400 ± 1°C in T-shaped pyrex tubes sealed under high vacuum ($\approx 10^{-6}$ Torr). The volatile products were collected in a cold trap while the surface-bound products were removed from the silica as the corresponding phenols by basic digestion and then silylated to form trimethylsilyl ethers. The samples were analyzed by capillary GC with flame ionization detection or by GC-MS. Quantitative measurements were made with the use of internal standards and measured GC detector response factors.

RESULTS AND DISCUSSION

Thermolysis of ~~DPB at 400°C has been studied at 2-12% conversion with two high coverage batches, 0.541 mmol/g (Batch A) and 0.504 mmol/g (Batch B). At the lowest conversion (ca. 2% in 10 min), the major gas phase products of the cracking reaction detected in the cold trap were toluene (PhMe), ethylbenzene (PhEt), styrene (PhVi), and allylbenzene (PhAll). The surface-attached products obtained as phenols from basic digestion of the sample were *p*-cresol (corresponding to ~~PhMe), *p*-ethylphenol (~~PhEt), *p*-hydroxystyrene (~~PhVi), and *p*-hydroxyallylbenzene (~~PhAll). These eight products (shown in eq. 1) account for >97% of the products formed at 2% conversion and 93% at 12% conversion. The product distribution for the four gas phase hydrocarbon products, which will be examined in more detail below, is shown as a function of conversion in Figure 1. The two high coverage batches gave similar product distributions with reaction rates slightly faster for Batch B (ca. 15%).

$$\sim\sim PhCH_2CH_2CH_2CH_2Ph \rightarrow \begin{cases} \sim\sim PhCH_3 + PhCH_2CH{=}CH_2 \\ \sim\sim PhCH_2CH_3 + PhCH{=}CH_2 \\ \sim\sim PhCH{=}CH_2 + PhCH_2CH_3 \\ \sim\sim PhCH_2CH{=}CH_2 + PhCH_3 \end{cases} \qquad (1)$$

As conversion of ~~DPB increased, secondary products formed at the expense of the surface-bound olefinic products. At the highest conversion studied (12%), 7.0 mol% of the products results from secondary reactions. The major secondary reactions appear to be rearrangement of $\sim\sim PhCH_2CH{=}CH_2$ to $\sim\sim PhCH{=}CHCH_3$ (2.6 mol %), and radical addition to ~~PhVi and ~~PhAll to produce, following hydrogen abstraction, $\sim\sim PhCH_2CH_2CH_2Ph$ (0.6 mol %), $\sim\sim PhCH_2CH_2CH_2Ph\sim\sim$ (0.7 mol %; identified as the corresponding diphenol), $\sim\sim PhCH_2CH_2CH_2CH_2Ph\sim\sim$ (0.5 mol %), and isomers of $\sim\sim C_{24}H_{24}\sim\sim$ (1.0 mol %; diphenols of triphenylhexane). Comparable secondary radical addition reactions have been reported to occur during thermolysis of liquid DPB.[5]

Thermolysis of liquid 1,4-diphenylbutane (DPB) has been shown to proceed by a radical chain decomposition reaction in which DPB is cracked to give four major products, as shown in equation 2.[5]

$$PhCH_2CH_2CH_2CH_2Ph \rightarrow PhCH_3 + PhCH_2CH{=}CH_2 + PhCH_2CH_3 + PhCH{=}CH_2 \qquad (2)$$

By comparison, surface-immobilized DPB reacted to form the same set of gas phase products as well as a corresponding set of surface-attached products (eq. 1). This results from the nonequivalence of the two ends of the surface-attached DPB molecule. Therefore, at low conversion, liquid DPB and ~~DPB react in an analogous manner to produce the same slate of products. The initial rate of ~~DPB thermolysis at high coverage ($15 \pm 2\%\ h^{-1}$ at 400°C based on 2-12% conversion) is somewhat faster than that of liquid DPB. Comparison of the rate of reaction of liquid DPB and ~~DPB at 400°C for 10 min shows that the surface-immobilized DPB reacts 10-fold faster. It is also interesting that while the rate of decomposition of liquid DPB exhibited a mildly autocatalytic behavior, the rate of ~~DPB decomposition calculated at each time point was independent of conversion. Additional studies will probe these observations further and examine the dependence of the thermolysis rate on surface coverage.

In the radical chain propagation steps for the decomposition of DPB, a benzyl radical (or a 2-phenylethyl radical) abstracts a hydrogen atom from DPB in a competitive process to form a benzylic and a nonbenzylic diphenylbutyl radical (eqs. 3 and 4). The β-scission of the benzylic radical leads to PhVi and ultimately PhEt, while the nonbenzylic radical leads to PhAll and ultimately PhMe (eqs. 5 and 6).

$$PhCH_2CH_2CH_2CH_2Ph + PhCH_2\bullet \text{ (or } PhCH_2CH_2\bullet) \rightarrow$$
$$PhC\bullet HCH_2CH_2CH_2Ph + PhCH_3 \text{ (or } PhCH_2CH_3) \quad (3)$$

$$PhCH_2CH_2CH_2CH_2Ph + PhCH_2\bullet \text{ (or } PhCH_2CH_2\bullet) \rightarrow$$
$$PhCH_2C\bullet HCH_2CH_2Ph + PhCH_3 \text{ (or } PhCH_2CH_3) \quad (4)$$

$$PhC\bullet HCH_2CH_2CH_2Ph \rightarrow PhCH{=}CH_2 + PhCH_2CH_2\bullet \quad (5)$$

$$PhCH_2C\bullet HCH_2CH_2Ph \rightarrow PhCH_2CH{=}CH_2 + PhCH_2\bullet \quad (6)$$

In the case of ~~DPB, there are four different methylene units which can form two distinct benzylic (1 and 4) and two distinct nonbenzylic (2 and 3) radicals. Following initiation by the homolysis of a small amount of ~~DPB, the β-scission steps of the four possible radicals formed by hydrogen abstraction are shown in equations 7-10.

$$\underset{1}{\sim\sim PhC\bullet HCH_2CH_2CH_2Ph} \rightarrow \sim\sim PhCH{=}CH_2 + PhCH_2CH_2\bullet \quad (7)$$

$$\underset{2}{\sim\sim PhCH_2C\bullet HCH_2CH_2Ph} \rightarrow \sim\sim PhCH_2CH{=}CH_2 + PhCH_2\bullet \quad (8)$$

$$\underset{3}{\sim\sim PhCH_2CH_2C\bullet HCH_2Ph} \rightarrow \sim\sim PhCH_2\bullet + PhCH_2CH{=}CH_2 \quad (9)$$

$$\underset{4}{\sim\sim PhCH_2CH_2CH_2C\bullet HPh} \rightarrow \sim\sim PhCH_2CH_2\bullet + PhCH{=}CH_2 \quad (10)$$

The free and surface-bound radicals can propagate the chain by reacting with ~~DPB to form free and surface-bound PhMe and PhEt while regenerating the surface-bound DPB radicals.

The regioselectivity for thermolysis of fluid phase DPB was found to be concentration dependent.[5] This was explained by a substrate-dependent hydrogen abstraction reaction which interconverts the benzylic and the nonbenzylic radicals, equation 11.

$$PhC\bullet HCH_2CH_2CH_2Ph + PhCH_2CH_2CH_2CH_2Ph =$$
$$PhCH_2CH_2CH_2CH_2Ph + PhCH_2C\bullet HCH_2CH_2Ph \quad (11)$$

In the neat liquid at 400°C, conditions under which the reaction in eq. 11 occurs efficiently, the regioselectivity of thermolysis as determined from the PhEt/PhMe ratio extrapolated to zero conversion, was a minimum of 1.22. Interestingly for ~~DPB at 400°C, the analogous regioselectivity for formation of 1 relative to 2, determined from the PhEt/PhMe ratio, at 2% conversion is 1.23, while the benzylic/nonbenzylic selectivity for the pair farthest from the surface (4 relative

to 3), determined from the PhVi/PhAll ratio, is a somewhat smaller value of 1.08. These observations suggest that hydrogen exchange reactions on the surface analogous to eq. 11 may also be important for surface-immobilized ~~DPB at high coverage.

The selectivity for formation of benzylic radicals 4 and 1 can be probed by the PhVi to PhEt yield ratio since these products are not consumed by secondary reactions. At low conversions (2%), the ratio has a value of 1.0 indicating no selectivity, but as the conversion increases, the ratio increases to 1.2 at 12% conversion. A similar type of conversion dependent selectivity for the benzylic radical farthest from the surface has been reported in the thermolysis of ~~DPP at saturation coverages in which the selectivity varied from 1.0 at <4% conversion to 1.3 at 23% conversion. The explanation for this conversion dependent regioselectivity for ~~DPB lies in the hydrogen transfer propagation step. As the conversion increases, ~~DPB molecules are increasingly separated from the surface-bound hydrogen abstracting benzylic and 2-phenylethyl radicals, and hydrogen abstraction at the benzylic carbon farthest from the surface to form radical 4 becomes favored. Additional insight into this regioselectivity should be obtained from the current studies being performed at lower surface coverages.

CONCLUSIONS

Covalent attachment of organics to an inert support has proven useful in modeling the effects of the restricted radical mobility in the thermal reactions of coal related model compounds. Thermolysis of surface-immobilized 1,4-diphenylbutane at 400°C was found to proceed through a facile free radical chain decay pathway giving products analogous to those found in the thermolysis of liquid DPB, but with a somewhat faster rate. For ~~DPB at low conversions, there is little regioselectivity between the four radical chain decay pathways which cycle through radicals at benzylic and nonbenzylic methylene sites suggesting that a hydrogen exchange reaction may be important at high surfaces coverages. At the highest conversion studied (12%), the cracking favors hydrogen abstraction from the benzylic carbon farthest from the surface. Additional studies are in progress to examine the effects of lower surface coverages on the regioselectivity and rate of the thermal cracking of ~~DPB. The results from thermolysis of ~~DPP and ~~DPB support the idea that a free radical chain induced decomposition reaction can be an effective mechanism for the mild thermal degradation of polymethylene chains connecting aromatic moieties in coal even under conditions of restricted diffusion.

ACKNOWLEDGMENTS

This research was sponsored by the Division of Chemical Sciences, Office of Basic Energy Sciences, U.S. Department of Energy, under contract DE-AC05-840R21400 with Martin Marietta Energy Systems, Inc.

REFERENCES

1. (a) Whitehurst, D. D. *ACS Symp. Ser.* 1978, 1. (b) Schlosberg, R. H., Ed. *Chemistry in Coal Conversion,* Plenum: New York, 1985.

2. Elliott, M. A., Ed. *Chemistry of Coal Utilization,* Wiley-Interscience: New York, 1981; Suppl. Vol. 2: (a) Howard, J. B., Chapter 12. (b) Gorin, E., Chapter 27.

3. Buchanan, III, A. C.; Dunstan, T. D. J.; Douglas, E. C.; Poutsma, M. L. *J. Am. Chem. Soc.* **1986**, *108*, 7703.

4. (a) Buchanan, III, A. C.; Biggs, C. A. *Prepr., Am. Chem. Soc., Div. Fuel Chem.* **1987**, *32 (3)*, 175. (b) Buchanan, III, A. C., Biggs, C. A. *J. Org. Chem.*, in press.

5. Poutsma, M. L.; Dyer, C. W. *J. Org. Chem.* **1982**, *47*, 4093.

Figure 1. Thermolysis of ~~Ph(CH2)4Ph

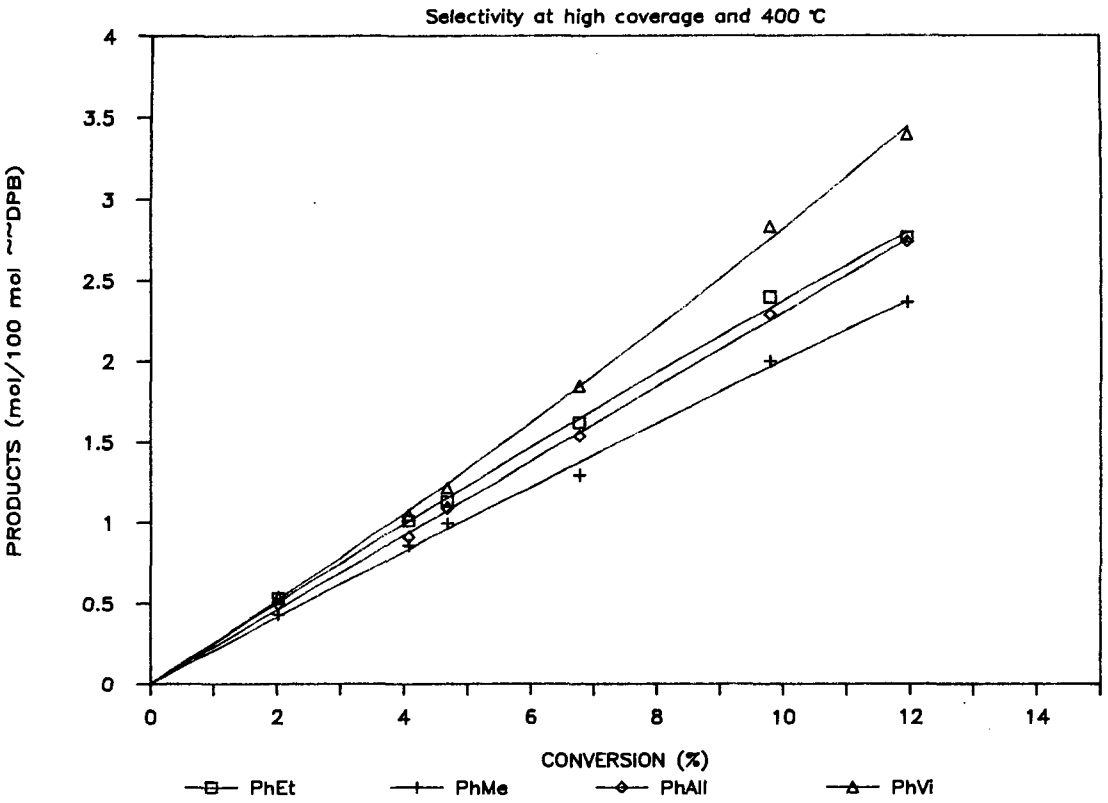

THE LUBRICITY PROPERTIES OF JET FUEL AS A FUNCTION OF COMPOSITION PART 1: METHOD DEVELOPMENT

Bruce H. Black[a], and Dennis R. Hardy

CODE 6180, Naval Research Laboratory, Washington, DC 20375-5000
[a]GEO-Centers, Inc., Fort Washington, MD 20744

ABSTRACT

In recent years, the quality of petroleum feedstocks used by refineries has decreased. This has necessitated the use of severe refinery processes in order to produce jet fuels of high thermal stability and cleanliness. Unfortunately, these processes remove naturally occurring polar material which impart a fuel's inherent lubricity. As a result, the lubricity properties of jet fuel products have decreased. This critical fuel property is essential for sustained high performance of fuel lubricated engine components. This paper describes a method that correlates naturally occurring and added carboxylic acids with fuel lubricity as measured by the Ball-on-Cylinder Lubricity Evaluator (BOCLE).

INTRODUCTION

In recent years, the quality of petroleum feedstocks has decreased. Thus, it has become necessary to employ severe refining processes in order to produce jet fuels of high thermal stability and cleanliness. Processes such as hydrotreating, hydrocracking, and clay filtering effectively remove the compounds which decrease thermal stability and hinder water removal by coalescence.[1-4] Unfortunately, some of these compounds are believed to impart a fuel's natural lubricity. Removal of these compounds, therefore, leads to a decrease in the operational lifetime of fuel lubricated engine components in some military and commercial aircraft. This in turn causes increased maintenance costs and down-time of aircraft. For the commercial airlines, this can cause a loss of revenue while an aircraft is grounded. For the military, this can lead to a decreased state of readiness.

Lubricity is a qualitative description of the relative abilities of two fluids, with the same viscosity, to limit wear and friction between moving metal surfaces.[2,4] It may be the most critical fuel property degraded by refinery processes.[5,6] There have been instances where the use of low lubricity fuel has caused loss of aircraft and human life.[7]

Considerable effort has been made in the development of a mechanical method which can be performed in the laboratory which will measure fuel lubricity. The current and most widely accepted method is the Ball-on-Cylinder Lubricity Evaluator (BOCLE). The lubricity of a fuel is determined by the measurement of a wear scar on a ball which has been in contact with a rotating cylinder partially immersed in a fuel sample. The reported value is the average of the major and the minor axes of the oval wear scar in millimeters. Typical values for jet fuels are between 0.45

and 0.95 mm.

This paper describes a method for estimating the lubricity properties of jet fuel by compositional analysis. The information developed by this technique is compared to measurements of the same fuels on the BOCLE. The method is based on a previously developed method for determining the concentration of corrosion inhibitor as a lubricity enhancer additive in fuel.[8-10] The analysis procedure involves a base extraction of a fuel sample with subsequent analysis by high resolution size exclusion chromatography. The amount of naturally occurring organic acids extracted from the fuels correlate well with their respective BOCLE measurements.

EXPERIMENTAL

Reagents- HPLC grade uninhibited tetrahydrofuran (THF) and HPLC grade methylene chloride were obtained from Fisher Scientific. Six test fuels and a hydrocarbon standard used for BOCLE repeatability and reproducibility studies were obtained from the Naval Air Propulsion Center, Trenton, NJ. These samples included: two JP-4 fuels, one of which had been clay filtered; two Jet A fuels, one of which had been clay filtered; a JP-5 fuel; a JP-7 fuel; and ISOPAR M, an isoparaffinic fluid used as a low lubricity standard. A model JP-5 fuel was prepared using technical grade (99.7% purity) n-dodecane obtained from Phillips 66 Co. HPLC grade toluene was obtained from Burdick and Jackson Laboratories Inc. Other constituents of the model fuel were obtained from Fisher Scientific. These compounds included indan, decalin, t-butylbenzene, and cyclohexylbenzene. To investigate the effect of organic acid type on lubricity enhancement, the following acids were used: octanoic, decanoic, lauric, palmitic, stearic, cyclohexane carboxylic acid, and dodecylbenzene sulfonic acid.

Equipment and Materials- Samples were analyzed using a Beckman-Altex Microspherogel high resolution, size exclusion column, Model 255-80 (50A pore size, 30cm x 8.0mm I.D.). Uninhibited THF was used as the mobile phase. The THF was periodically sparged with dry nitrogen to inhibit formation of hazardous peroxides. The injector was a Rheodyne Model 7125. A Beckman Model 100-A HPLC pump was used for solvent delivery with a Waters Model 401 differential refractometer for detection. Peaks were identified using a Varian Model 9176 strip chart recorder. A Fisher Accumet pH Meter Model 610A and a Fisher Standard Combination Electrode Catalog Number 13-639-90 were used for pH adjustments. BOCLE measurements were performed at twenty different laboratories worldwide. The BOCLE used was an InterAv Model BOC 100. The cylinders used were Timken Rings Part Number F25061 obtained from the Falex Corp., Aurora, IL. The test balls used were 12.7mm diameter, SKF Swedish Steel, Part Number 310995A obtained from SKF Industries, Allentown, PA.

Method- Fuel samples were analyzed for organic acid concentration by a previously developed method.[8] For each sample, 100 ml were extracted with 100 ml of 0.2M aqueous sodium hydroxide. The aqueous phase was drained into a clean beaker and acidified dropwise with concentrated hydrochloric acid. The pH of the aqueous solution was lowered to 2.0 ± 0.03. The acidified aqueous phase was back-extracted with 100 ml HPLC

grade methylene chloride. The methylene chloride was drained into a clean beaker and allowed to evaporate. After evaporation, the residue was dissolved in 2.0 ml HPLC grade THF and transferred to a glass vial with a teflon-lined cap.

BOCLE measurements on the seven fuel samples were performed in duplicate at twenty laboratories in the United States and Europe. The BOCLE method used was according to appendix Y of the Aviation Fuel Lubricity Evaluation published by the Coordinating Research Council, Inc.[11] The lubricity of each sample was measured using both a 500 and a 1000 gram load for the ball on cylinder. The compositional analysis data is correlated with the 500 gram load BOCLE data.

To determine the effect of sulfonic acid on lubricity enhancement, six model fuel samples were prepared for BOCLE analysis. These samples are listed with their relative wear scar diameter measurements in Table 1.

RESULTS

Figures 1 and 2 are size exclusion chromatograms for the seven fuel samples. Figure 1 represents those fuels which were determined to have high lubricity. Figure 2 represents those fuels which were found to have low lubricity. The region of interest on the chromatogram is the area where retention volume is between 5.25 ml and 7.5 ml. The peaks which elute after 7.5 ml are artifacts and were not extracted from the fuel. In Figures 1a and 1b, the peaks with retention volumes less than 6.25 ml correspond to the presence of the lubricity enhancer additive. The peak which elutes at approximately 5.85 ml represents the major active ingredient in most commercial additives, dilinoleic acid (DLA). It has a molecular weight of 562 daltons. This material is prepared by a 1,4-cycloaddition (Diels-Alder) reaction of two linoleic acid molecules. The product is a monocyclic compound with a molecular weight twice that of linoleic acid. It possesses two carboxylic acid groups which are believed to be the points of adsorption to active surface sites.

The small peak which elutes at approximately 5.4 ml corresponds to the presence of trilinoleic acid (TLA). TLA, which is also a product of the Diels-Alder reaction, may possess either a partially unsaturated fused dicyclic ring structure or two isolated partially saturated cyclohexyl rings. It has a molecular weight approximately three times that of linoleic acid (840 daltons).

The fuels whose chromatograms are depicted in Figures 1c and, Figures 2a through 2d, do not possess the lubricity enhancer additive. Their lubricity properties are, for the most part, solely related to the presence of naturally occurring carboxylic acids. The correlation of acidic materials present which elute at 7.25 ml is made with the BOCLE measurements. This retention volume was arbitrarily chosen because it was representative of naturally occurring organic acids present in each of the samples.

Table 2 lists the BOCLE results of the seven fuel samples. Statistically, it can be seen that there are two distinct groups. Three

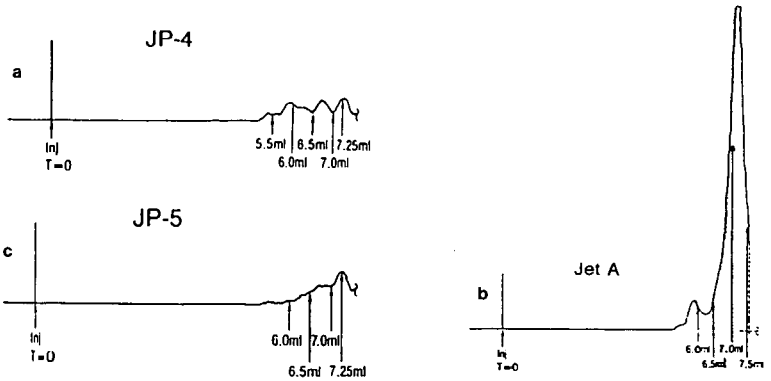

FIGURE 1: HPLC Chromatograms of High Lubricity Fuels as Determined by the Ball-on-Cylinder Lubricity Evaluator.

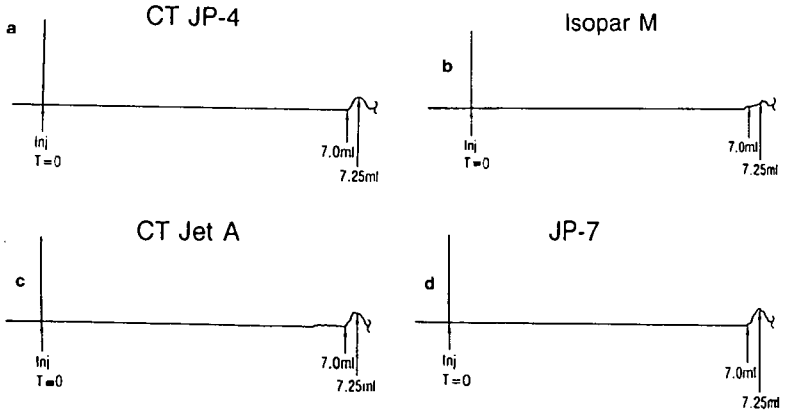

FIGURE 2: HPLC Chromatograms of Low Lubricity Fuels as Determined by the Ball-on-Cylinder Lubricity Evaluator.

fuels, JP-4, Jet A, and JP-5, were found to have high lubricity, and the four others, clay filtered JP-4, ISOPAR M, clay filtered Jet A, and JP-7, were found to have low lubricity. The results within each set are statistically the same. The average relative wear scar diameter for the high lubricity fuels is 0.64 mm ± 0.05 mm (7.8%). The average relative wear scar diameter for the low lubricity fuels is 0.94 ± 0.10 mm (10.6%). This implies that the precision of the BOCLE is better for high lubricity rather than low lubricity fuels.

Table 3 compares the the peak height at 7.25 ml with the BOCLE measurements for each of the fuels. Both JP-4 and Jet A possess the lubricity enhancer additive. It is, therefore, not surprising that these were high lubricity fuels. It can be seen in Figure 1b and Table 3 that the Jet A sample had a significantly higher concentration of the naturally occurring carboxylic acids and lubricity enhancer additive than either the JP-4 or JP-5. The lubricity of the Jet A, however, was not significantly higher than the other high lubricity fuels. Previous work has shown that there is a minimum possible wear scar diameter. The addition of more lubricity enhancer additive or the presence of a greater amount of naturally occurring lubricity enhancing species will not decrease the wear scar diameter.[11] In each of the high lubricity fuels, the maximum lubricity has been achieved. Thus, the lubricity measurements for these fuels are the same.

There may be some question as to why the JP-5 sample had significantly higher lubricity than the four low lubricity fuels. In Table 3, it can been seen that the JP-5 sample has only twice the concentration of acidic species eluting at 7.25 ml than the low lubricity fuels, yet the lubricity properties are significantly better. By comparison of Figure 1c with Figures 2a through 2d, it can be seen that each of the fuels in Figure 2 possess a single peak which elutes at 7.25 ml. The JP-5 sample depicted in Figure 1c has, not only this peak, but higher molecular weight acidic species which elute between 6.25 and 7.0 ml. We propose that the presence of these naturally occurring components in addition to two to three times the concentration of material eluting at 7.25 ml, yields the higher lubricity characteristics.

Dodecylbenzene sulfonic acid (DBSA) was found to have no effect on lubricity at concentrations that are normally found in jet fuel. Table 1 shows that at DBSA concentrations up to 1.0 ppm, DBSA did not decrease wear scar diameter measurements for the model fuel. This is in agreement with work performed by Lazarenko, et al. They found that corrosion inhibitors based on sulfonic acids did not increase jet fuel lubricity.[14] Model fuel doped with 96.0 ppm of a carboxylic acid mixture had, however, significantly lower wear scar diameter measurements, i.e., lubricity had increased as expected.

DISCUSSION AND CONCLUSIONS

The effect of long chain carboxylic acids on boundary lubriciation is well established. The presence of naturally occurring long chain carboxylic acids in jet fuel is believed to play a major role in lubricity enhancement. Any refinery procedure which removes these acids will have a

detrimental effect on the lubricity of jet fuel products. Thus, processes such as hydrotreatment, hydrocracking, and clay filtration will decrease jet fuel lubricity.

It is well known that clay filtration adversely affects jet fuel lubricity. It has long been believed that this is a result of the removal of naturally occurring polar materials in fuel which impart lubricity.[2,3,7,12,13] The results of the BOCLE measurements confirm that lubricity does indeed decrease after clay filtration. The compositional changes can be seen by comparison of Figures 1b and 2c which represent Jet A fuel before and after clay filtration. The concentration of lubricity imparting organic acids has been drastically reduced. The lubricity enhancer additive has also been completely removed. The corresponding result is an extreme reduction in fuel lubricity. Comparison between clay filtered and non-clay filtered JP-4 cannot be made since these were two different fuels. It can be seen, however, that the mandatory corrosion inhibitor/lubricity enhancer additive is not present in the clay filtered sample.

This work has shown that a direct relationship between the presence of naturally occurring carboxylic acids and BOCLE measurements exists. Previous work by has also shown this relationship.[8] They analyzed a series of additive-free JP-5 and Jet A samples for naturally organic acids and correlated their presence with the fuels' respective BOCLE measurements. Additional work, which will be published in a subsequent paper, has shown the relationship in Naval JP-5 field samples as well as Air Force JP-4 field samples.

Sulfonic acids, however, were not found to influence BOCLE measurements and, therefore, do not enhance lubricity. Other polar material in jet fuel may contribute to lubricity enhancement. The carboxylic acids, which are well known surface active and lubricity enhancing species, are likely to be the major contributor.

In the future, it appears as though the BOCLE will be accepted as the standard method for measuring lubricity in the laboratory. The compositional analysis method can be used as a supplementary method to the BOCLE for verification of lubricity measurements. There are, however, a few advantages to the compositional analysis method over the BOCLE. First, the BOCLE is operator sensitive. Second, the instrument is sensitive to contamination of the fuels and test materials. Third, the presence of dissolved oxygen and water in a sample will influence the wear scar generated. Fourth, the BOCLE is very sensitive to relative humidity.

The compositional analysis method is not sensitive to relative humidity or dissolved oxygen and water in a fuel sample. Trace contamination between samples does not occur as readily with the compositional analysis method and its influence is significantly less. The compositional analysis method is also able to distinguish between three types of high lubricity fuel which the BOCLE cannot. These include; a high lubricity fuel without corrosion inhibitor, a high lubricity fuel with corrosion inhibitor, and a low lubricity fuel with corrosion inhibitor.

Although the lubricity enhancer additive is mandatory in U.S. military

jet fuel, a number of Naval JP-5 fuel samples were indentified where the lubricity additive may not have been necessary. Addition of the lubricity enhancer additive to these fuels may have been an unnecessary expense. In addition, the lubricity enhancer additive has been shown to adversely effect the removal of water from fuel by coalescence. The use of the additive, therfore, may actually be detrimental rather than beneficial in some fuels.

Finally, for those fuels which have had the lubricity enhancer additive blended in at the refinery, the compositional analysis method can be used as a quality assurance and quality control procedure. Both the refiner and user can analyze a fuel for levels of both naturally occurring and added lubricity imparting organic acids.

TABLE 1

SAMPLE	Conc. DBSA (ppm)	Conc. R-COOH (ppm)	Normalized WSD
1	0.0	0.0	0.99
2	0.5	0.0	0.98
3	1.0	0.0	1.00
4	0.0	96.0	0.49
5	0.5	96.0	0.51
6	1.0	96.0	0.53

The Effect of Dodecylbenzene Sulfonic Acid on Lubricity as Measured by the BOCLE in the Presence and Absence of Carboxylic Acids.

TABLE 2

SAMPLE	Normalized WSD	± 2σ
JP-4	0.63	0.05
JET A	0.64	0.05
JP-5	0.65	0.05
CT JP-4	0.92	0.11
ISOPAR M	0.93	0.09
CT JET A	0.93	0.09
JP-7	1.00	0.11

The Lubricity of Fuel Samples as Measured by the Ball-on-Cylinder Lubricity Evaluator.

TABLE 3

SAMPLE	Normalized WSD	Pk Hgt @ 7.25 mL
JP-4*	0.63	10.0 mm
JET A*	0.64	>165.0 mm
JP-5	0.65	**15.5 mm
CT JP-4	0.92	6.5 mm
ISOPAR M	0.93	4.5 mm
CT JET A	0.93	6.0 mm
JP-7	1.00	7.5 mm

*Contained a lubricity enhancer additive
**Higher molecular weight acidic species were also present

The Comparison of Organic Acid Composition at 7.25 mL Retention Volume with Lubricity as Measured by the Ball-on-Cylinder Lubricity Evaluator.

REFERENCES

1. Vere, R. A. Soc. Automot. Eng., SAE Reprint Number 690667, National Aeronautic and Space Engineering and Manufacturing Meeting, Los Angeles, CA, October, 1969; pp 2237-2244.
2. Moses, C. A.; Callahan, T. J.; Cuellar, Jr., J. P.; Dodge, L. G.; Likos, W. E.; Naegeli, D. W.; Valtierra, M. L. "An Alternative Test Procedure to Qualify Fuels for Navy Aircraft"; Final Report, Naval Air Propulsion Center Contract Number N00140-80-C-2269, Report Number NAPC-PE-145C; Southwest Research Institute, San Antonio, TX, 1984.
3. Petrarca, Jr., J. "Lubricity of Jet A-1 and JP-4 Fuels"; NTIS Number AD-784772; Report Number AFAPL-TR-74-15, Air Force Aero Propulsion Laboratory, Wright-Patterson AFB, OH, 1974.
4. Goodger, E.; Vere, R. Aviation Fuels Technology; MacMillan Publishers Ltd.: Houndmills, Basingstoke, Hampshire, England, 1985; pp 80-82.
5. Biddle, T. B.; Meehan, R. J.; Warner, P. A. "Standardization of Lubricity Test"; Report Number AFWAL-TR-87-2041, Air Force Wright Aeronautical Laboratories, Aero Propulsion Laboratory (AFWAL/POSF), Wright-Patterson AFB, OH, 1987.
6. Master, A. I.; Weston, J. L.; Biddle, T. B.; Clark, J. A.; Gratton, M.; Graves, C. B.; Rone, G. M.; Stoner, C. D. "Additional Development of the Alternative Test Procedure for Navy Aircraft Fuels"; Naval Air Propulsion Center Contract Number N00140-84-C-5533, Report Number NAPC-PE-160C; United Technologies Corporation, Pratt and Whitney, West Palm Beach, FL, 1987.
7. Fishman, E.; Mach, M. H.; Fraser, L. M.; Moore, D. P. "Navy Mobility Fuels Evaluation"; Final Report, Naval Research Laboratory Contract Number N00014-82-C-2370; TRW Energy Technology Division, Redondo Beach, CA, 20 July 1984.
8. Black, B. H.; Wechter, M. A.; Hardy, D. R. J. Chromatogr. 1988, 437, 203-210.
9. Hardy, D. R.; Black, B. H.; Wechter, M. A. J. Chromatogr. 1986, 366, 351-361.
10. Wechter, M. A. "Quantitative Determination of Corrosion Inhibitor Levels in Jet Fuels by HPLC"; Final Report, Naval Research Laboratory Contract Number N00014-85-M-0248; Southeastern Massachusetts University, North Dartmouth, MA 1986.
11. Coordinating Research Council "Aviation Fuel Lubricity Evaluation"; CRC Report Number 560, CRC Inc., Atlanta, GA, 1988.
12. Grabel, L. "Lubricity Properties of High Temperature Jet Fuel"; NTIS Number AD-A045467; Report Number NAPTC-PE-112, Naval Air Propulsion Test Center, Trenton, NJ, 1977.
13. Grabel, L. "Effect of Corrosion Inhibitors on the Lubricity and WSIM of JP-5 Fuels"; Interim Report Number NAPC-LR-80-7, Naval Air Propulsion Center, Trenton, NJ, 1980.
14. Lazarenko, V. P.; Skorvorodin, G. B.; Rozhkov, I. V.; Sablina, Z. A.; Churshukov, E. S. Chemistry and Technology of Fuels and Oils 1975, 11, No. 5 & 6, 356-359.

THE LUBRICITY PROPERTIES OF JET FUEL AS A FUNCTION OF COMPOSITION PART 2: APPLICATION OF ANALYSIS METHOD

Bruce H. Black[a], and Dennis R. Hardy

CODE 6180, Naval Research Laboratory, Washington, DC 20375-5000
[a]GEO-Centers, Inc., Fort Washington, MD 20744

ABSTRACT

In recent years, the quality of petroleum feedstocks used by refineries has decreased. This has necessitated the use of severe refinery processes in order to produce jet fuels of high thermal stability and cleanliness. These processes, however, tend to decrease the lubricity properties of jet fuel products. As a result, fuel lubricated engine components have been experiencing greater wear and mechanical failure. To alleviate this problem, a highly effective lubricity enhancer additive, based on mixtures of carboxylic acids, is mandatory in all U.S. military jet fuel. The additive, however, has been shown to interfere with the removal of water from jet fuel by coalescence. In addition, some fuels possess high levels of naturally occurring, lubricity enhancing carboxylic acids and, therefore, do not need the additive. This paper describes the application of an analysis method that distinguishes between fuels with and without the additive, and fuels that possess naturally occurring, lubricity enhancing carboxylic acids.

INTRODUCTION

In part 1 of this work, it was shown that a direct correlation exists between the presence of naturally occurring carboxylic acids and Ball-on-Cylinder Lubricity Evaluator (BOCLE) measurements.[1] This correlation was applied to a series of fuel samples that were used to determine the repeatability and reproducibility of the BOCLE instrument. Extensive BOCLE data had been generated to which the compositional analysis results could be compared. The compositional analysis method was found to be able to distinguish between naturally occurring and added lubricity enhancing carboxylic acids.

This paper applies the compositional analysis method to a series of Navy JP-5 jet fuel samples obtained from a worldwide survey of storage depots. BOCLE measurements were performed at the Naval Air Propulsion Center (NAPC), Trenton, NJ. As in the previous work, the presence of carboxylic acids in a fuel sample increased its inherent lubricity. The compositional analysis method also identified fuels which were deficient in the mandatory lubricity enhancer additive.

EXPERIMENTAL

Reagents- HPLC grade uninhibited tetrahydrofuran (THF) and HPLC grade methylene chloride were obtained from Fisher Scientific. Seven JP-5 fuel

samples, from the Navy's Second Worldwide Fuel Survey, were obtained from the Naval Air Propulsion Center.

Equipment and Materials- Samples were analyzed using a Beckman-Altex Microspherogel high resolution, size exclusion column, Model 255-80 (50A pore size, 30cm x 8.0mm I.D.). Uninhibited THF was used as the mobile phase. The THF was periodically sparged with dry nitrogen to inhibit formation of hazardous peroxides. The injector was a Rheodyne Model 7125. A Beckman Model 100-A HPLC pump was used for solvent delivery with a Waters Model 401 differential refractometer for detection. Peaks were identified using a Varian Model 9176 strip chart recorder. A Fisher Accumet pH meter Model 610A and a Fisher standard combination electrode Catalog Number 13-639-90 were used for pH adjustments. An Interav Model BOC 100 Ball-on-Cylinder Lubricity Evaluator was used for lubricity measurements. The cylinders were 100% spheroidized annealed bar stock, consumable vacuum melted AMS 6444 steel obtained from Jayna Enterprises, Inc., Vandalia, OH. The balls used were 12.7mm diameter, SKF Swedish Steel, Part Number 310995A obtained from SKF Industries, Allentown, PA.

Method- Fuel samples were analyzed for carboxylic acid concentration by a previously developed method.[2] For each sample, 100 ml were extracted with 100 ml of 0.2M aqueous sodium hydroxide. The aqueous phase was drained into a clean beaker and acidified dropwise with concentrated hydrochloric acid. The pH of the aqueous phase was lowered to pH 2.0 ± 0.03. The acidified aqueous phase was back-extracted with 100 ml HPLC grade methylene chloride. The methylene chloride was drained into a clean beaker and allowed to evaporate. After evaporation, the residue remaining was dissolved in 2.0 ml HPLC grade THF and transferred to a glass vial with a teflon-lined cap.

BOCLE measurements were performed in triplicate on each of the fuel samples. The method used was according to appendix Q of the Aviation Fuel Lubricity Evaluation published by the Coordinating Research Council, Inc.[3] The sum of the values obtained for each sample was averaged and the relative wear scar diameter measurements are reported in Table 1.

RESULTS AND DISCUSSION

As in previous work, the presence of carboxylic acids, both naturally occurring and added, correlates well with BOCLE measurements. The relative average wear scar diameter for each sample is listed in Table 1. The cylinders used for this work were somewhat softer than the Timken rings previously used in Part 1 of this work. As a result, the actual wear scar diameter measurements were somewhat lower with a narrower range.

It can be seen in Table 1 that five of the seven fuels analyzed possessed the lubricity enhancer additive. Four of these fuels had both the major constituent, dilinoleic acid (DLA), and a minor component present in some lubricity enhancer additives, trilinoleic acid (TLA). Two of the fuels analyzed, however, did not possess any appreciable amount of the mandatory lubricity enhancer additive.

In Figures 1 through 5, the major lubricity enhancer additive

component, DLA, elutes at approximately 5.85 ml. The DLA component has a molecular weight of about 560 daltons. This material is prepared by a 1,4-cycloaddition (Diels-Alder) reaction of two linoleic acid molecules. The product is a monocyclic compound with a molecular weight twice that of linoleic acid. It possesses two carboxylic acid moieties which are believed to be the points of attachment to active surface sites.

In Figures 1 through 4, the peak corresponding to the TLA component is also present. This component elutes at approxmately 5.4 ml. The TLA component, which is also a product of the Diels-Alder reaction, has a molecular weight of approximately 840 daltons. It may possess either a partially unsaturated fused dicyclic ring structure or two isolated partially saturated cyclohexyl rings.

As expected, the fuels that possess the lubricity enhancer additive were found to have the highest lubricity. Those fuels that did not possess the lubricity enhancer additive, and were also deficient in naturally occurring carboxylic acids, were found to have the lowest lubricity. From what is known about carboxylic acids with respect to lubricity enhancement, continued use of these fuels could lead to lubricity related problems.

Table 2 lists the peak heights for the added and naturally occurring carboxylic acids extracted from the fuel samples. Fuel samples 1 through 3 each possessed similar amounts of the lubricity enhancer additive. Fuel sample 4 had slightly less than the first three fuel samples, while fuel 5 was devoid of the TLA component and had significantly less of the DLA component. Two sets of data for the naturally occurring carboxylic acids are listed. In previous work, it was found that some fuels possess two distinct molecular weight ranges of naturally occurring carboxylic acids.[1,2] These two ranges are designated regions 3 and 4. These components have retention volumes of approximately 6.5 and 7.0ml respectively and can be clearly seen in Figure 3.

High resolution, size exclusion chromatography separates components on the basis of molecular shape and size and, therefore, to an extent, molecular weight. In general, one would expect a normal distribution of straight chain alkanoic acids which parallels the distribution of normal alkanes present in a fuel. The presence of two separate peaks for the naturally occurring carboxylic acids indicates the presence of two distinct classes of constituents. Region 3 corresponds to the straight chain alkanoic acids, while region 4 corresponds to mono- and polycylic carboxylic acids. The maxima for regions 3 and 4 correspond to the molecular weight of tetradecanoic acid (C_{14}), and octanoic acid (C_8) respectively. The condensed size of a cyclic compound, as opposed to a straight chain compound, yields a calculated molecular weight lower than its actual molecular weight. For this reason, region 4 is most likely comprised of not only monocyclic carboxylic acids, but polycyclic acids as well.

Maxima for regions 3 and 4 are not as well defined in other fuels examined. For these fuels, the height was measured at a retention volume that corresponds to the maxima in Figure 3. In Figures 1, 2, and 5, the concentration of carboxylic acids present in region 3 increased gradually as the molecular weight decreased. In each case, there is a very rapid

increase in carboxylic acid concentration in the region 4 molecular weight range. Similar results were found in earlier work.[1,2]

In each fuel previously examined, there was some minimum amount of carboxylic acids present in region 4. Not all fuels, however, possessed the carboxylic acids which correspond to region 3. Some had very low concentrations, some had approximately equal concentrations. These differences may be a result of crude source, refinery operations, or storage conditions.

CONCLUSIONS

The compositional analysis method has been applied to a series of field samples to determine the presence of naturally occurring and added carboxylic acids are known to enhance jet fuel lubricity. The concentration present in a given fuel sample correlates well with its inherent lubricity as measured by the BOCLE.

A number of molecular weight ranges of carboxylic acids are present in most jet fuels. Two of these regions correspond to the presence of an added lubricity enhancer, and two or more correspond to naturally occurring lubricity enhancing carboxylic acids. The relative effectiveness of each region has not yet been determined. It is believed, however, that the dimer of linoleic acid is more effective than the trimer. This is a result of steric hindrance between trimer molecules when attached to surfaces.[4-6]

The relative effectiveness of the naturally occurring carboxylic acids is believed to increase as chain length increases. Daniel found that, in general, the ease of adsorption increases with increasing chain length.[7] Boundary lubrication also increases as chain length increases.[8,9] The lubricity properties of jet fuel, therefore, may increase as the presence of longer chain carboxylic acids increases. At some point, however, there is probably a limit to lubricity enhancement by increasing chain length. The relative effectiveness of region 3 over region 4, therefore, may be substantially different due to the differences in structure.

There may be some question as to why the mandatory lubricity enhancer additive is absent from two of the fuels examined. There are possible explanations for this. First, the lubricity enhancer additive was originally added to the fuel to inhibit corrosion to fuel handling and storage systems which resulted from dissolved oxygen and free-water present in fuel. The carboxylic acid based corrosion inhibitors were serendipitously found to enhance the lubricity properties of low lubricity fuels.[10-13] As lubricity related problems became more prevalent, the primary purpose for the corrosion inhibitor was lubricity enhancement. Unfortunately, the military specification for jet fuel was not modified to include lubricity properites. Second, the additives are accepted and used, not for their ability to enhance lubricity, but to inhibit corrosion. Some of these additive are based on acylated glycols and acylated alkanolamines. the compositional analysis method described in this paper is not suitable for analysis of these materials. It should be noted that

these materials have been shown to be relatively ineffective lubricity enhancers. Third, the additive was not added at the refinery as it should have been.Additive loss due to adsorption in fuel handling has been found to be insignificant. Previous work has shown that as little as 3% is lost due to adsorption on the surfaces of a 100 mile pipeline.[14]

The compositional analysis method can be used as a supplement to the BOCLE. The BOCLE can determine if a fuel has sufficient lubricity characteristics. The compositional analysis method can determine if the lubricity is a result of naturally occurring or added carboxylic acids or both.

REFERENCES

(1) Black, B. H.; Hardy, D. R. "The Lubricity Properties of Jet Fuel as a Function of Composition: Part 1- Correlation of Fuel Composition with Ball-on-Cylinder Lubricity Evaluator (BOCLE) Measurements"; Submitted for Publication in Energy and Fuels, 1988.

(2) Black, B. H.; Wechter, M. A.; Hardy, D. R. J Chromatogr. 1988, 437, 203-210.

(3) Coordinating Research Council "Aviation Fuel Lubricity Evaluation"; CRC Report Number 560, CRC Inc., Atlanta, GA, 1988.

(4) Dacre, B.; Savory, B.; Wheeler, P. A. "Adsorption of Lubricity Additive Components, Part 1"; Technical Report AC/R/13 1977, Royal Military College of Science, Shrivenham, Swindon, Wiltshire, England; Contract Number AT/2160/025/ENG D, Procurement Executive, Ministry of Defense, London.

(5) Dacre, B.; Wheeler, P. A.; Savory B. "Adsorption of Lubricity Additive Components, Part 2"; Technical Report AC/R/30 1979, Royal Military College of Science, Shrivenham, Swindon, Wiltshire, England; Contract Number AT/2160/025/ENG D, Procurement Executive, Ministry of Defense, London.

(6) Dacre, B.; Wheeler, P. A.; "Adsorption of Lubricity Additive Components, Part 3- Kinetics of Adsorption"; Technical Report AC/R/33 1980, Royal Military College of Science, Shrivenham, Swindon, Wiltshire, England; Contract Number AT/2160/025, Procurement Executive, Ministry of Defense, London.

(7) Daniel, S. G. Trans. Faraday Soc. 1944, 47, 1345-1359.

(8) Allen, C. M.; Drauglis, E. Wear 1969, 14, 363-384.

(9) Levine, O.; Zisman, W. A. J. Phys. Chem. 1957, 61, 1188-1200.

(10) Vere, R. A. Soc. Automot. Eng., SAE Reprint Number 690667, National Aeronautic and Space Engineering and Manufacturing Meeting, Los Angeles, CA, October, 1969; pp 2237-2244.

(11) Petrarca, Jr., J. "Lubricity of Jet A-1 and JP-4 Fuels"; NTIS Number AD-784772; Report Number AFAPL-TR-74-15, Air Force Aero Propulsion Laboratory, Wright-Patterson AFB, OH, 1974.

(12) Martel, C. R.; Bradley, R. P.; McCoy, J. R.; Petrarca, Jr., J. "Aircraft Engine Turbine Corrosion Inhibitors and Their Effects on Fuel Properties"; NTIS Number AD-787191; Report Number AFAPL-TR-74-20, Air Force Aero Propulsion Laboratory, Wright-Patterson AFB, OH, 1974.

(13) Grabel, L. "Lubricity Properties of High Temperature Jet Fuel"; NTIS Number AD-A045467; Report Number NAPTC-PE-112, Naval Air Propulsion Test Center, Trenton, NJ, 1977.

(14) Black, B.H.; Hardy, D.R.; Wechter, M.A. "The Determination and Use of Isothermal Adsorption Constants of Jet Fuel Lubricity Enhancer Additives"; Ind. Eng. Chem. Res., In Review, 1988.

TABLE 1

SAMPLE	Relative WSD	TLA Present	DLA Present
1. Roosevelt Roads, P.R.	0.67	YES	YES
2. Guantanamo, Cuba	0.70	YES	YES
3. Diego Garcia	0.71	YES	YES
4. Iorizaki, Japan	0.77	YES	YES
5. Gatun, Panama	0.79	NO	YES
6. Cartagena, Spain	0.86	NO	NO
7. Azores	1.00	NO	NO

The Relative Lubricity of Fuel Samples as Measured by the Ball-on-Cylinder Lubricity Evaluator.

TABLE 2

SAMPLE	TLA Pk Hgt	DLA Pk Hgt	Reg. 3 Pk Hgt	Reg. 4 Pk Hgt
1	4.0	15.5	14.5	126.0
2	4.0	15.0	11.0	25.0
3	4.0	16.0	20.0	22.0
4	1.5	11.0	4.0	3.5
5	0.0	7.5	12.0	74.0
6	0.0	0.0	5.0	8.5
7	0.0	0.0	7.5	6.5

The Results of the Compostional Analysis of Fuel Samples for Natural and Added Carboxylic Acids.

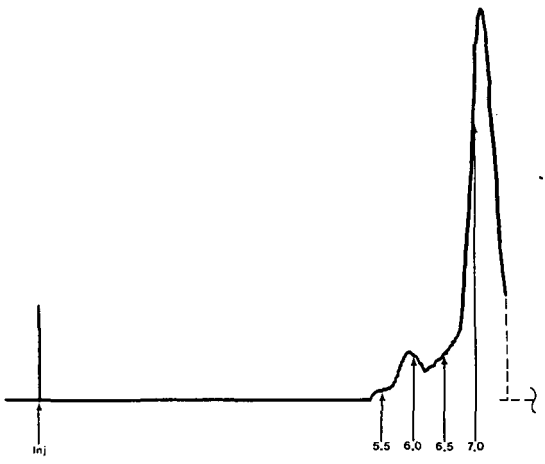

FIGURE 1: HPLC Chromatogram of Base Extracted JP-5 Jet Fuel from Roosevelt Roads, Puerto Rico.

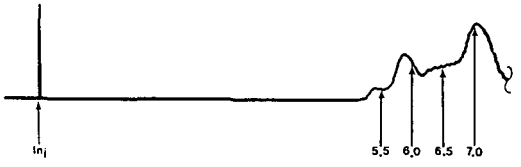

FIGURE 2: HPLC Chromatogram of Base Extracted JP-5 Jet Fuel from Guantanamo, Cuba.

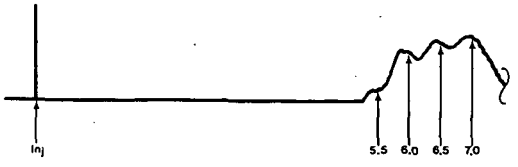

FIGURE 3: HPLC Chromatogram of Base Extracted JP-5 Jet Fuel from Diego Garcia.

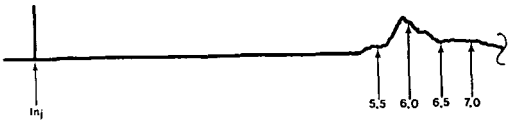

FIGURE 4: HPLC Chromatogram of Base Extracted JP-5 Jet Fuel from Iorizaki, Japan.

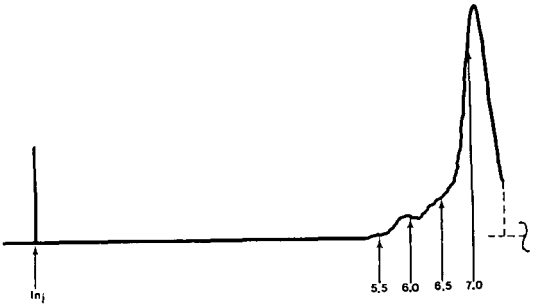

FIGURE 5: HPLC Chromatogram of Base Extracted JP-5 Jet Fuel from Gatun, Panama.

FIGURE 6: HPLC Chromatogram of Base Extracted JP-5 Jet Fuel From Cartagena, Spain.

FIGURE 7: HPLC Chromatogram of Base Extracted JP-5 Jet Fuel from the Azores.

ALKALI AND ALKALINE EARTH PROMOTED CATALYSTS FOR COAL LIQUEFACTION APPLICATIONS

Anastasios Papaioannou and Henry W. Haynes, Jr.
Department of Chemical Engineering
University of Wyoming
P. O. Box 3295, University Station
Laramie, WY 82071

INTRODUCTION

The promotion of Co (or Ni) Mo/Alumina hydrotreating catalysts with percentage quantities of alkali and alkaline earth metals has been proposed as a means of reducing carbon formation when the catalyst is subjected to a high coking environment (1, 2, 3). We recently reported the results of a study in which a sodium promoted NiMo catalyst was compared with the untreated catalyst while hydrotreating a coal-derived liquid (4). In terms of hydrogenation activity, the treated and untreated catalysts were essentially equivalent. Both possessed excellent activity and this activity was well maintained over the 400 hour run duration. Carbon deposition on the used catalyst was substantially reduced by the sodium treatment. The incorporation of sodium into the catalyst did, however, reduce the hydrodenitrogenation activity. The present study was undertaken to ascertain whether similar effects could be realized by promotion with the alkaline earth metals.

EXPERIMENTAL

Catalyst deactivation runs were conducted in the bench scale trickle bed hydrotreater described previously (4). The reactor is charged with only three grams of catalyst, and at this scale of operation it is difficult to obtain reliable kinetics information due principally to the low liquid mass velocities characteristic of such systems (5). One should therefore not attach too much significance to the absolute values of the reported rate constants. Rather it is the relative values of the rate constants that is significant. The system has proven to be a reliable catalyst screening tool as the data are reproducible and conditions are chosen such that differences in activity level are readily observed.

The catalyst selected for this investigation is a CoMo/Alumina catalyst (Amocat 1A-nominal 16 wt% MoO_3, 3 wt% CoO) provided by the Amoco Oil Company. This catalyst was designed specifically for coal liquefaction applications as described in (6, 7). A calcium promoted catalyst was prepared from the Amocat 1A by the incipient wetness impregnation with aqueous calcium nitrate followed by calcining for four hours at 450°C. The finished catalyst contained 5.3 wt% CaO. A magnesium promoted catalyst (3.8 wt% MgO) was prepared similarly. Both weight percentages correspond to a loading of 0.9 mole alkaline earth per mole molybdenum. Properties of all three catalysts are summarized in Table I. The catalysts were sulfided in 10% H_2S/H_2 prior to characterization.

The feedstock employed in this investigation is a mildly hydrogenated creosote oil (560-835°F) spiked with 20 wt% ash free coal liquid vacuum bottoms (1000$^+$°F) obtained from the Advanced Coal Liquefaction Research Facility at Wilsonville, Alabama, Run 247. Properties of the feedstock HCO1-R are compiled in Table II.

Crude kinetics models were developed for the HCO1-R/Amocat 1A feedstock/catalyst system in a manner similar to the procedure described by Baker, et al. (4). Details are provided in a final DOE report (8). The hydrogen uptake kinetics are first order reversible; whereas, the hydrodenitrogenation kinetics are taken to be first order and irreversible. Deactivation run conditions are summarized in Table III. These conditions, while severe by hydrotreating standards, are not out of line when compared to coal liquefaction conditions.

BET surface areas were calculated from the nitrogen adsorption isotherm at liquid nitrogen temperatures. Pore size distributions were obtained by mercury porosimetry. Prior to characterization, all used catalysts were extracted in tetrahydrofuran (THF) for 24 hours and dried under vacuum at 100°C for 48 hours. The used THF extracted catalysts were analyzed for carbon-hydrogen content in a combustion tube apparatus. All catalysts were subjected to acid sites characterization by the Temperature Programmed Desorption (TPD) of t-butylamine (9, 10). We calculate a Relative Acid Density (RAD) by dividing the high temperature "β-peak" area by the BET surface area. This quantity is an indication of the acid sites density when compared with other catalysts in the program. Attempts to interpret the maximum peak temperature as a measure of acid site strength are complicated by the decomposition of the adsorbed base prior to its desorption from the sample (11).

RESULTS AND DISCUSSION

Hydrogen uptake deactivation curves for the three catalysts are plotted in Figure 1. While there may have been some loss in day one activity due to the addition of promotor metals, it seems clear that the hydrogenation activities are essentially equivalent after the first few hours on stream. Similar results were observed in an earlier study of sodium promoted catalysts (4). In contrast the hydrodenitrogenation activities are significantly lowered by the incorporation of alkaline earth metals into the catalyst, Figure 2. (An upset was experienced prior to the last balance period during the run with unpromoted catalyst, hence the dashed line.) Furthermore, the reduction in activity appears to be related to catalyst acidity as can be ascertained from the RAD values in Table I. The most acidic catalyst, i.e. the unpromoted catalyst, possesses the highest hydrodenitrogenation activity; whereas, the least acidic Ca-promoted catalyst exhibits the lowest activity. The Mg-promoted catalyst lies in between these extremes with regard to both acid site density and hydrodenitrogenation activity. It appears that acid sites are essential for good hydrodenitrogenation activity presumably because they provide preferential adsorption sites for basic nitrogen species. Acid sites are evidently not essential for good hydrogenation activity, however.

Properties of the used THF extracted catalysts are compiled in Table IV. By comparison with the fresh catalyst values of Table I, it is apparent that a modest reduction in surface area has occurred with the greatest reduction being for the untreated catalyst. The loss in pore volume is more substantial with the pore volume reduction ranging from 33% for the Ca-promoted catalyst to 49% for the unpromoted catalyst. This is also evident from a comparison of cumulative pore size distributions plotted in Figures 3 and 4.

The most interesting information in Table IV is the carbon deposition data. Indeed promotion with alkaline earth metals does serve to reduce coke deposition. Calcium promotion is more effective than magnesium promotion, and again the results suggest that coke deposition may be related to catalyst acidity.

Higher coke levels are observed on the more acidic catalysts.

The results of this study are broadly consistent with recent results reported by Shimada and coworkers (12). These investigators also observed that doping with Ca and Mg served to reduce both coke level and hydrodenitrogenation activity. Consistent with previous results for sodium promoted catalysts (13) they find that activity losses are reduced by adding the alkaline earth metal as a last step in the preparation, i.e. after the active metals have been added. Somewhat contrary to our findings is their observation that hydrogenation activity is also reduced by the alkaline earth treatment. However, it may be important to note that this conclusion is based on the hydrogenation of a model compound in a batch reactor. Their results thus reflect initial activity levels. As noted above our initial hydrogenation activity appears to be higher for the unpromoted catalyst, but after a few hours on stream this advantage disappears. Similar results were obtained with sodium promoted catalysts (4).

Our results for both alkali (4) and alkaline earth promoted hydrotreating catalysts have been explained in a rather straightforward manner in terms of catalyst acidity. However, in a study of hydrotreating catalysts prepared on different support materials (14), we report findings that appear somewhat contradictory of the present results. In particular we observe a trend of decreasing coke formation with increasing RAD. This may be due to the fact that characterization of catalyst acidity by TPD of t-butylamine is far from complete. In particular, our analysis provides little or no information regarding the strength (11) or type (Bronsted or Lewis) of acidity. These factors may be expected to effect both coking tendency and activity levels.

CONCLUSIONS

The promotion of an otherwise finished CoMo/Alumina hydrotreating catalyst with percentage quantities of alkaline earth metals offers an effective means of reducing coking tendency while maintaining a high hydrogenation activity. The treatment does have an adverse affect on hydrodenitrogenation activity. Alkali and alkaline earth promotion may therefore be beneficial in applications such as coal liquefaction where the primary function of the catalyst is to hydrogenate and the reaction environment is conducive to coking.

ACKNOWLEDGEMENTS

This work was jointly sponsored by the U.S. Department of Energy (Grant DE-FG22-88PC88942) and the Amoco Oil Company. We are grateful for both the financial support and the helpful consultations provided by these organizations.

REFERENCES

1. Kelly, J.F. and M. Ternan, Can. J. Chem. Eng. 57, 726 (1979).

2. Kelly, J.F.; Kriz, J.F. and M. Ternan, Canadian Pat. No. 1,121,293, April 6, 1982.

3. Kageyama, Y. and T. Masuyama, "Hydrogenation Catalysis of Coal Liquid Bottoms", Proc. 1985 Int. Conf. Coal Sci., Sidney, Oct. 28-31, 1985.

4. Baker, J.R.; McCormick, R.L. and H.W. Haynes, Jr., I & EC Res. 26, 1895 (1987).

5. Satterfield, C.N., AIChE Jour. 21, 209 (1975).

6. Bertolacini, R.J.; Gutberlet, L.C.; Kim, D.K. and K.K. Robinson, "Catalyst Development for Coal Liquefaction", Final Rept. AF-1084, EPRI, June 1979.

7. Kim, D.K.; Bertolacini, R.J.; Forgac, J.M.; Pellet, R.J.; Robinson, K.K. and C.V. McDaniel, "Catalyst Development for Coal Liquefaction", Final Rept. AF-1233, EPRI, Nov. 1979.

8. Haynes, H.W. Jr., "Improved Catalysts for Coal Liquefaction", Final Rept. DOE/PC/70812-13, USDOE, April, 1988.

9. Mieville, R.L. and B.L. Meyers, J. Catal. 74, 196 (1982).

10. Nelson, H.C.; Lussier, R.J. and M.E. Still, Appl. Catal. 7, 113 (1983).

11. McCormick, R.L.; Baker, J.R.; Haynes, H.W. Jr. and R. Malhotra, Energy & Fuels 2, 740 (1988).

12. Shimada, H.; Sato, T; Yoshimura, Y.; Nishijima, A.; Matsuda, M.; Konakahara, T. and K. Sato, Sekiyu Gakkaishi 31, 227 (1988).

13. Boorman, P.M.; Kriz, J.F.; Brown, J.R. and M. Ternan, Proc. 4th Climax Int. Conf. Chem. and Uses of Molybdenum, 192 (1982).

14. McCormick, R.L.; King, J.A.; King, T.R. and H.W. Haynes, Jr., "The Influence of Support on the Performance of Coal-Liquids Hydrotreating Catalysts", sub. to I & EC Res., 1988.

Table I

Fresh Catalyst Properties

	Amocat 1A	Mg-Promoted	Ca-Promoted
BET Surface Area, m^2/g	167	144	135
Pore Volume (> 60 Å dia.), cc/g	0.71	0.69	0.69
Avg. Micropore Diameter, Å	130	125	125
Avg. Macropore Diameter, Å	4500	4500	4500
Relative Acid Density, m^{-2}	0.049	0.036	0

Table II

Feedstock Properties (HCO1-R)

wt% C	91.43
wt% H	6.84
wt% S	0.20
wt% N	0.68
wt% O (BD)	0.85
wt% Asphaltene	12
wt% Preasphaltene	4
Sp. Gr. (60/60 F)	1.1232

Table III

Nominal Deactivation Run Conditions

Pressure =	2000 psig
Temperature =	440°C (825°F)
WHSV =	3.0
H_2 Treat Rate =	5500 SCF/BBL

Table IV

Used Catalyst Properties

	Amocat 1A	Mg-Promoted	Ca-Promoted
BET Surface Area, m^2/g	137	137	118
Pore Volume (> 60 Å dia.), cc/g	0.36	0.41	0.46
Avg. Micropore Diameter, Å	100	100	100
Avg. Macropore Diameter, Å	4000	4100	4100
Relative Acid Density, m^{-2}	0.020	0.014	0
Wt% Carbon	17.2	13.2	9.80
Wt% Hydrogen	1.34	1.01	1.03

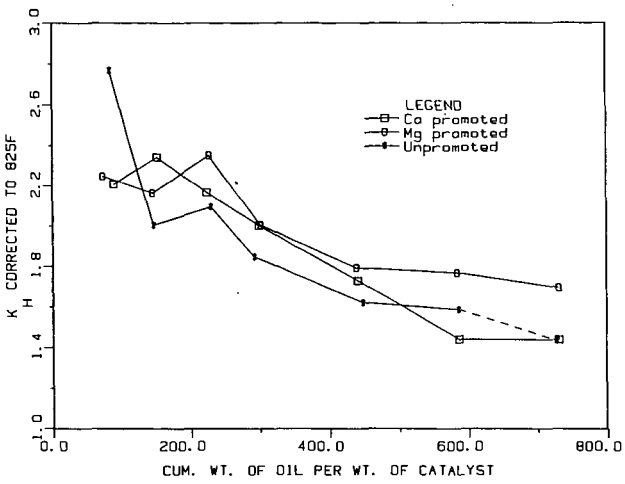

Figure 1. Deactivation curves for hydrogen uptake.

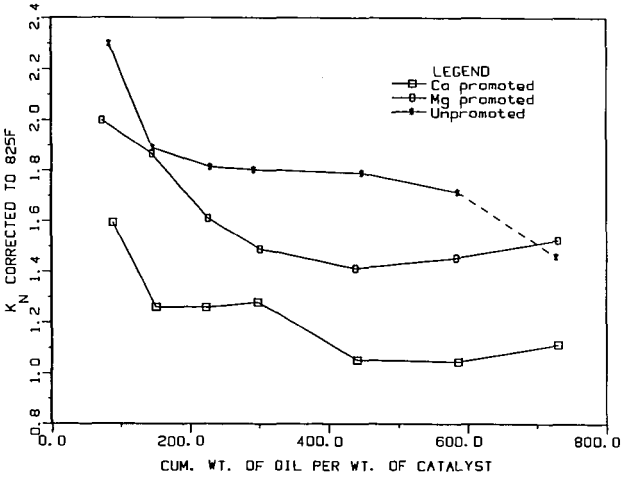

Figure 2. Deactivation curves for hydrodenitrogenation.

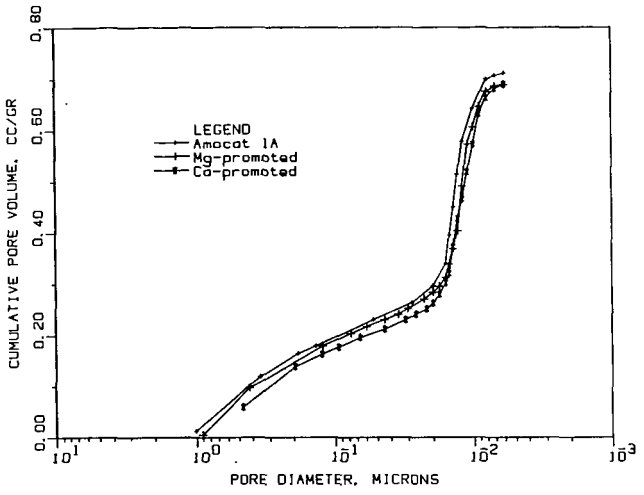

Figure 3. Cumulative pore size distributions for fresh catalysts.

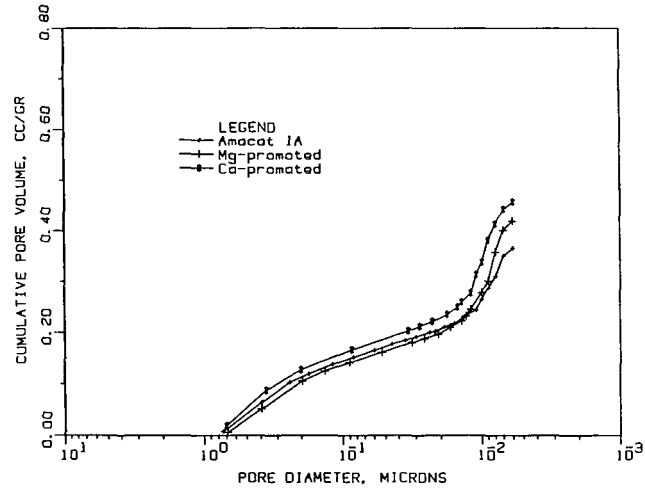

Figure 4. Cumulative pore size distributions for used catalysts.

REACTIONS OF LOW-RANK COALS WITH PHENOL

Edwin S. Olson, Ramesh K. Sharma, and John W. Diehl
University of North Dakota Energy and Mineral Research Center
Box 8213 University Station, Grand Forks, ND 58202

Although the acid-catalyzed reaction of coals with phenol has been investigated for some time, the nature of the products, especially with respect to molecular weights, remains unclear. Heredy investigated the reaction of coals with phenol and boron trifluoride at 100°C, with the objective of selectively degrading the coal macromolecules so that monomeric units could be isolated (1,2). The resulting product from a high volatile bituminous coal was claimed to be soluble to a large extent (61% in phenol). The definition of solubility, however, was simply that the phenol extract was filtered through Celite. The particle size was not measured nor was the absence of a Tyndall effect noted. Molecular weight measurements were carried out on various fractions by ebullioscopic measurements in benzene, benzene-methanol or pyridine. The molecular weight of the phenol soluble material was reported to be 1150 daltons using pyridine ebullioscopy. The chemistry of the reaction is believed to be a transalkylation of the methylene bridging group between two aromatic systems onto a molecule of the phenol. A substantial amount of phenol was chemically incorporated into the products resulting from the treatment.

Stating the same objective as Heredy, Ouchi (3) reacted coals with phenol and p-toluenesulfonic acid as the catalyst at 185°C. Pyridine Soxhlet extraction of the product from a Yubari coal (84.6% C, 6.1% H) resulted in high yields of material. Molecular weights as measured by pyridine boiling point elevation were less than 500.

These acid-catalyzed transalkylation reactions with phenol appear to fragment the macromolecular network of the coals to give extracts which the phenol solvent alone cannot give. The question of the colloidal nature of the extract has been addressed by Larsen (4,5) and Sharma (6). Since the pyridine extracts were found to plug 0.5 micron filters, a significant amount of the material in the extract was colloidal. Centrifugation at 120,000 x g for three hours precipitated the colloidal material. The actual amount of colloidal material present varied with the coal, but was as high as 80%. Gel permeation chromatography of the "truly soluble" material with VPO measurement of collected fractions gave a molecular weight (M_n) distribution which indicated that most of the material had a molecular weight greater than 6000. The early-eluting material appeared to be highly polydisperse, hence the VPO measurements were likely to be inaccurate and overly influenced by the smaller molecular weight material present (7). The conclusion of Larsen was that the soluble products were very large molecules and only limited depolymerization had occurred.

Although Givens's and Larsen's observations and arguments are persuasive, reports of alleged depolymerization continue to appear in the literature. Ouchi (8) has recently claimed to have depolymerized an Austrailian (Yallourn) brown coal, while advancing the argument that a low-rank coal should behave differently toward the phenolation reaction than the higher rank coals investigated by Larsen. Unfortunately Ouchi did not address the colloidal nature of the products and inappropriately used VPO and size exclusion chromatography for the determination of molecular weights. Thus, his number average molecular weight value of 1120 daltons for the pyridine extract of the product cannot be taken seriously.

The objective of our investigations was to determine the extent to which the cross linking methylene units between aromatic systems are broken down in low-rank coals (Wyodak and Yallourn) during the phenolation reaction with p-toluenesulfonic acid and compare the results with those from the reaction with a bituminous coal. In order to determine the extent of depolymerization, the weight average molecular weight of the products were examined using Rayleigh light scattering. Thus the range of molecular weights above 6000 which were not accessible in Larsen's experiments can be accurately measured with this technique.

EXPERIMENTAL

Phenolation: Wyodak coal (C, 70,9; H, 5.2: N, 0.92; S, 0.60; O, 22.3; maf basis), Yallourn brown coal (C, 69.4; H, 4.9; N, 0.6; S, 0.3; O, 24.8), and Pittsburgh #8 coal (C, 82.0; H, 5.5; N, 2.0; S, 6.8; O,3.7) were demineralized by heating and stirring for three hours with 1N HCl, filtered and washed with water until free of acid, and dried in vacuum at 110°C for 24 hours. Phenol and p-toluenesulfonic acid monohydrate were heated with the coals according to Ouchi's procedure (8). The reaction products were worked up by distillation in vacuo until the volume was reduced to about one-third. The product was poured into a large excess of water, stirred for 2 hours and filtered. The residue was washed with water until free of acid and steam distilled to remove residual phenol. Last traces of phenol were removed by heating the residue in vacuo at 110° until constant weight was obtained.

The dried products were extracted with pyridine using Soxhlet extraction under dry nitrogen until there was no color observable in the solvent. The pyridine extract was concentrated to about one third its volume and added to a large excess of 1 N hydrochloric acid and stirred for 3 hours. The precipitate was filtered, washed repeatedly with 1 N hydrochloric acid and then with water until free of acid, and dried in vacuo at 110°C to a constant weight.

Reductive acetylation: The pyridine-soluble phenolation products were reductively acetylated by the method used for humic acids (9). Molecular weight determinations of the reductively acetylated products in THF were carried out as previously described with a KMX-6 low angle laser light scattering photometer (9).

RESULTS

The coals dispersed in the refluxing phenol and acid catalyst (p-toluenesulfonic acid) giving high yields of products. The weight of the product was greater than the weight of starting coal, as described in earlier papers, due to chemical combination of the phenol with the coal. The phenol uptake was inversely proportional to the coal rank. The weight increase for Yallourn brown coal was 86%, whereas the Wyodak subbituminous coal exhibited a 65% weight increase, and for the Pittsburgh #8, a 47% increase was observed.

The infrared spectra of the phenolation products were obtained by photoacoustic spectroscopy and exhibit evidence for the incorporation of phenol; that is, strong O-H, aromatic ring and ether stretching absorptions. The ether stretching absorption could be due to the formation of ethers by a dehydration reaction occurring under these conditions; however, further work is needed to establish the nature of the incorporated phenol in these products.

A large fraction of the phenolated coals became dispersible in pyridine. The penolation product from Yallourn brown coal was 97% dispersed, the Wyodak product was 87% dispersed and the Pittsburgh #8 products was 84% dispersed. As observed

by Larsen, attempted filtration of the pyridine dispersions using a 0.5 micron Millipore filter resulted in plugging. Thus these products in pyridine should be regarded as organosols or colloids as suggested by Larsen, not as true solutions.

The objective of this study was really to determine the size of the macromolecules making up this dispersion by conversion of the coal-derived material to a soluble form so that we could apply Rayleigh light scattering techniques, which are appropriate for large macromolecules and do not rely on calibration with small molecular species. This knowledge of the molecular weight of the entire fraction of product which is dispersible in pyridine is required for the determination of the extent of depolymerization of the coal in the phenolation reaction. The pyridine dispersed materials were only slightly soluble in THF, a solvent previously used effectively in low-angle laser light scattering photometry (LALLS), and were highly colored, making observation of the Rayleigh scattering difficult.

In order to accomplish the molecular weight determination with LALLS, the pyridine-dispersed material was converted to a less polar and less colored form by reductive acetylation, as we had previously done with the humic acids from lignites. The yields of reductively-acetylated derivatives were nearly quantitative for the phenolation products from all three coals. Photoacoustic infrared spectra of these derivatives indicated complete absence of the hydroxyl stretching absorption and the presence of strong ester carbonyl absorption.

The reductively-acetylated material dissolved completely in THF and the resulting solution could be filtered through a 0.2 micron filter and did not exhibit the intense flashing (Tyndall effect) of the laser light by dispersed particulate matter. The THF solutions of the reductively-acetylated phenolation products had a lower molar absorptivity than the original phenolation products and the Rayleigh scattering could be easily observed.

Rayleigh scattering factors were measured for the dilute THF solutions of the reductively acetylated phenolation products, and corrected by means of the Cabannes factors which were determined for each of the solutions used. These corrected Rayleigh factors gave a linear reciprocal scattering plot (Kc/R_0 vs. c) with an r^2 of 0.99 for the coal derivatives. The weight average molecular weight of the reductively acetylated Wyodak product was 1.67 million daltons, as determined from the intercept of the reciprocal plot. The slope was positive ($A_2 = 3.0 \times 10^{-3}$). The reductively acetylated phenolation product from the Yallourn brown coal had a molecular weight of 2.26 million daltons ($A_2 = 1.3 \times 10^{-3}$). The weight average molecular weight of the reductively acetylated phenolation product from the Pittsburgh #8 was 2.23 million with an A_2 of 4.6×10^{-3}.

DISCUSSION

Molecular weight determinations of derivatives of the phenolation products from both high and low rank coals gave high values in the light scattering determination. These reductively acetylated derivatives of the phenolation products gave true solutions in THF as defined by their ability to pass a 0.2 micron filter and the lack of a Tyndall effect in the laser beam. Furthermore the phenolation products were completely converted to this soluble form by the reductive acetylation, so the entire sample is being examined in the light scattering experiment. This contrasts with the Larsen experiment which separated the dispersed material out by ultracentrifugation and examined the soluble material by VPO, whose limitation in determining the high molecular weight material was discussed by Larsen. Ouchi (8) defined solubility as the lack of a

residue; this does not distinguish a true solution from a colloidal dispersion, and his molecular weight measurements are subject to the same limitations as Larsen's.

Because of the high molecular weights obtained, we conclude that both the low and high rank coals were not extensively depolymerized in the phenolation reaction. The reaction serves to cleave cross-linking bonds to create some mixture of soluble and dispersed particles, probably in the submicron range as in the dispersion obtained by treating Wyodak coal with sodium hydroxide. Thus cleavage of the guaiacyl ether linkages and possibly some activated methylene bridges will accomplish this limited digestion of the coal structure which does not amount to depolymerization or solubilization. Since the coal may not consist of repeating polymer units, perhaps a better generic term for the phenolation reaction is limited digestion or degradation.

The differences in the weight average molecular weights of the three coals may not be significant with respect to the coal structures, since extensive rearrangements of bonds and chemical adduction of phenol occurred in addition to cleavage of labile benzyl ether groups and methylene bridges between the aromatic systems. This complex reaction does not really allow us to count branch points or cross-links that are broken. One must proceed to other synoptic reactions to elucidate the types of cross links or branch points in these coals.

The differences in the second virial coefficient (A_2) obtained from the slope of the reciprocal Rayleigh plot for each coal phenolation product can be attributed to the differences in the Cabannes factors for the coal derivatives. The slope of a Cabannes factor vs. concentration plot is proportional to the coal rank; that is, the Cabannes factors increase more with concentration for the Pittsburgh #8 derivative than they do for the Wyodak, which in turn increase more than the Yallourn derivative. Thus, at higher concentrations the Rayleigh factors are more corrected and therefore proportionately smaller for the Pittsburgh #8 product, and the slope of the reciprocal plot is therefore greater. The high Cabannes factors are probably due to the presence of larger polynuclear ring systems in the product from the bituminous coal which result in greater anisotropic scattering.

REFERENCES

1. Heredy, L.A. and Neuworth, M.B. Fuel **1962**, 41, 221-31.
2. Heredy, L.A., Kostyo, A.E. and Neuworth, M.B. Fuel **1965**, 44 125-33.
3. Ouchi, K., Imuta, K. and Yamashita, Y. Fuel **1965**, 44, 29-38.
4. Larsen, J.W. and Lee, D. Fuel **1983**, 62, 918-23.
5. Larsen, J.W. and Choudhury, P. J.Org. Chem. **1979**, 2856-9.
6. Sharma, D.K. Fuel, **1988**, 67, 186-190.
7. Given, P.H. in Coal Science, Vol 3, ed by. Gorbaty, M.L., Larsen, J.W. and Wender,I. Academic Press, Orlando Florida, **1984**, 63-252.
8. Ouchi, K., Yokoyama, Y. Katoh, T. and Itoh, H. Fuel **1987**, 66, 1115-7.
9. Olson, E.S., Diehl, J.W. and Froehlich, M.L. Fuel, **1987**, 66, 992-5.

ACKNOWLEDGEMENTS

This research was supported by Contract No. DOE-FC21-86MC10637 from the U.S. Department of Energy. References herein to any specific commercial product by trade name or manufacturer does not necessarily constitute or imply its endorsement, recommendation, or favoring by the United States Government or any agency thereof.

LIQUEFACTION KINETICS INFLUENCED BY THE AMOUNT OF DONORS AND HYDROGEN PRESSURE

Isao Mochida, Ryuji Sakata and Kinya Sakanishi

Institute of Advanced Material Study, Kyushu University
Kasuga, Fukuoka 816, JAPAN

Abstract

Influences of donor and solvent amounts, hydrogen pressure and coal deashing on the product slate as well as rates of liquid production were studied in the hydrogen donating liquefaction of an Australian brown and a Japanese subbituminous coal using tetrahydrofluoranthene(4HFL) as a donor at 450 °C. An adequate amount of donor at the fixed solvent/coal ratio provided the best yield of oil plus asphaltene. The best amount varied, depending upon the coal and liquefaction conditions. Less amount of donor at the decreasing solvent/coal ratio gave much rapid decrease of the liquid yield. Hydrogen pressure around 40 kg/cm^2 certainly participated favorable in the liquefaction, especially pronounced at the low donor/coal ratio as observed with pyrolyses of model substrates. Deashing to remove dominant calcium ions was generally favorable to increase the liquid yield, however some coals at the low donor/coal ratio suffered some retrogressive reaction. Such results indicate multi-fold roles of solvent and plural mechanisms of coal-macromolecular depolymerization. Different reactivities of the brown coals of different lots are briefly discussed.

Introduction

Coal liquefaction process has been investigated for quite a time by examining various ideas to improve its efficiency[1-5]. Nevertheless, the process is still far away from satisfaction about the cost of product oil. Better yield of distillate oil on the bases of reactor volume, hydrogen consumption and very severe reaction conditions as well as fed coal is desperately wanted.

The macromolecular mixtures of solid coal are digested and/or depolymerized into distillable species through solvent extraction as well as pyrolytic, hydrogen-transferring and catalytic bond dissociations[6]. Poor interaction between the solid coal grain and solid catalyst, unless the fine catalysts are highly dispersed on the coal with rather extensive cost[7,8], suggests that the first step of coal conversion to obtain liquid easily accessible to the solid catalyst is dominated by the reactions among coal molecules, the solvent and gaseous atmosphere. It has been pointed that hydrogen donor solvents derived from 3-4 ring aromatic hydrocarbons are very powerful to liquefy the coal through their proper hydrogen-donating and dissolving abilities against coal molecules[9,10]. Thus, most appropriate use of donor solvent is an approach to find better scheme of coal liquefaction. The minimum amount of donor solvent to assure the maximum yield of oil and asphaltene may increase the efficiency of hydrogen consumption and the reactor volume, and moderates the conditions[11].

In addition to a classical mechanism of stabilization of thermally produced radicals from coal molecules, it has been recognized that donor molecules directly interact with the coal macromolecules to activate via hydrogenation and hydrocracking according to the reactivity of coal molecules as well as the donor, and reaction conditions[6, 11-13]. Such bimolecular mechanisms suggest the importance of the solvent quality and quantity under reaction conditions matched to the both materials for the liquefaction efficiency.

The hydrogen transferring mechanism may also suggest the importance of hydrogen pressure when the molecular hydrogen is activated by the radical species derived from donors and coal molecules. Vernon has pointed out the participation of molecular hydrogen in the pyrolysis of dibenzyl with the existence of tetralin[14]. The radical initiator is also suggested important to initiate the chain reactions of coal and solvent molecules according to the bimolecular mechanism.

In the present report, we are going to describe the influences of donor concentration in the solvent, donor amount and hydrogen pressure in the liquefaction of an Australian brown and a Japanese subbituminous coal on the yield of oil and asphaltene which are both easily converted into distillable clean oil by the successive catalytic hydrotreating process. Influences of such reaction variables were also studied with model substrates. The reactivity of the coals is very sensitive to the coagulation of their macromolecules and maceral composition[15]. Hence, the influence of deashing on the hydrogen-donating liquefaction and microscopic coal characterization were investigated[16,17]. Morwell brown coal is found to exhibit very different reactivity according to the rot, yielding variable amounts of asphaltene and residue.

Experimental

Materials

The ultimate analyses of the sample coals are summarized in Table 1. The liquefaction(hydrogen donating) solvent was tetrahydrofluoranthene(4HFL) prepared by catalytic hydrogenation of commercial fluoranthene(FL) using a commercial Ni-Mo catalyst in an autoclave at 250 °C, and quantified by g.c. and purified by recrystallization.

Pretreatment of coal

After the coal was ground to pass 60 US mesh screen, it was kept in refluxing aq. HCl(1N) and methanol(10 vol%) under nitrogen flow to remove divalent cations such as Ca^{2+}, Mg^{2+} and Fe^{2+}. After the pretreatment, the coal was filtered, washed with water, and dried in vacuum at room temperature.

Liquefaction procedure

Liquefaction was carried out in a tube bomb(20 ml volume). The coal(2.0 g), which had been ground to less than 60 US mesh and dried at 100 °C under vacuum, and the solvent(2.0, 3.0, 4.0 or 6.0 g), after their thorough mixing, were transferred to the bomb. The bomb was then pressurized with nitrogen or hydrogen gas to 1.0 or 2.0 MPa at room temperature and immersed into a molten tin bath at the prescribed temperature, and agitated axially. The

products remaining in the bomb were extracted with THF, benzene and n-hexane. The hexane soluble(HS), hexane insoluble-benzene soluble(HI-BS), benzene insoluble-THF soluble(BI-THFS) and THF insoluble(THFI) substances were defined as oil, asphaltene, preasphaltene and residue, respectively. Gas yield was calculated by the difference between the initial and recovered weight.

Results

Influences of 4HFL concentration in the fixed solvent/coal ratio of 3/1

Influences of 4HFL concentration on the product slate in the liquefaction of Morwell-I coal at 450 °C under nitrogen were shown in Table 2. The pure 4HFL solvent liquefied the coal very rapidly, whereas a longer reaction time increased markedly the gaseous product as well as the sum yield of oil and asphaltene. Although decreasing 4HFL in the solvent reduced the rates of liquefaction as for both gas and liquefied products, the 4HFL contents of 3/4 and 2/4 in the solvent provided more favorable product slates(high yield(>80%) of oil plus asphaltene and low yields of preasphaltene and gaseous products).

Influence of 4HFL(solvent)/coal ratio

Figure 1 illustrates the oil and asphaltene yields from Morwell-I coal at 450 °C under nitrogen for the respective best residence times using variable solvent(pure 4HFL)/coal ratios. The oil and asphaltene yields were only slightly influenced by the ratios to give around 60 and 10 % yields, respectively, when the ratio ranged from 3/1 to 1.5/1, although a trend of slight decreases of both yields may be observable with decreasing the ratios. Itis of value to point that the yields of preasphaltene and residue were always less than 5 %.

A drastic decrease of oil and hence the sum yield took place when the solvent/coal ratio was reduced to 1/1, while the significant increase of asphaltene with some increases of preasphaltene, residue and gas were observed at the best residence time of 10 min. The large increases of the latter three products were observed by a longer residence time at this ratio, resulting in a further marked decreases of objective products.

Influence of hydrogen pressure on coal liquefaction

Figure 2 illustrates the liquefaction yields from Morwell-I and -II coals at 450 °C and 1.5/1(4HFL/coal ratio) under nitrogen or hydrogen pressure. The conversion of asphaltene into oil was accelerated by hydrogen pressure, especially under higher pressure, where the interaction of molecular hydrogen with donor and/or coal molecules was enhanced. It should be noted that the highest oil yield from Morwell-II was achieved under higher hydrogen pressure at the reaction time of 20 min, when most of 4HFL was consumed.

Morwell-I was certainly more reactive than Morwell-II, giving higher oil yield regardless of atmosphere, although the sum yields of oil plus asphaltene were much the same. Lower reactivity of the asphaltene from Morwell-II coal is suggested.

Figure 3 illustrates the liquefaction yields from Taiheiyo

coal at 450 °C and 1.5/1(4HFL/coal ratio) under nitrogen or hydrogen pressure. Higher oil and aspahltene yield of 80 % was achieved from Taiheiyo coal than Morwell coals, reflecting much less gas yield. Pressure effect of hydrogen was marked at the reaction of 10 min, converting asphaltene into oil.

Influence of hydrogen pressure on the reaction of model compounds

Table 3 summarizes the influence of hydrogen pressure on the conversions of dibenzyl (DB) at 450 °C, 30 min and variable donor(4HFL)/substrate ratios. The conversions of DB were always higher under hydrogen pressure with less 4HFL consumption than those under nitrogen pressure. Such a tendency increases with decreacing 4HFL amount. It should be noted that hydrogen pressure enhanced the DB conversion even with a non-donor solvent.

Influence of deashing at low 4HFL/coal ratio

Figure 4 illustrates the liquefaction yields from the deashed Morwell-I and Taiheiyo coals at 450 °C-10 min and 1.5/1 (4HFL/coal ratio). The oil yield from Morwell-I coal increased to 65 % with decreasing gas, preasphaltene and residue yields. In contrast, the deashing pretreatment exhibited unfavorable effect on the lquefaction of Taiheiyo coal at low 4HFL/coal ratio, increasing the yields of gas and heavy fractions (preasphaltene and residue) with slight increase of oil yield.

Discussion

The present study revealed that the concentration and amount of donor, and hydrogen pressure are very influential on the yield of oil plus asphaltene in the hydrogen-transferring liquefaction. The volume of solvent defines the volume of reactor and its reduction can increase the productivity of the liquefaction.

The roles of solvent have been recognized multi-fold. The hydrogen donation performs the following reactions in coal liquefaction;

1. Stabilization of radicals derived thermally from the coal molecules.
2. Hydrogenation of reactive sites of coal molecules to loosen the bonds for their dissociation.
3. Cleavage of bonds in coal molecules by substitution with hydrogen atoms.

The contributions of these schemes are strongly dependent upon the reactivities of coal and solvent, and hence reaction conditions[11].

According to scheme 1, the coal liquefaction requires donor solvent over a certain quantity. Its excess amount stays unparticipated. Less amount fails to prevent the retrogressive reaction. In contrast, according to the schemes 2 and 3, the donor directly reacts with the coal molecules. Hence, its amount kinetically influences the liquefaction, more amount accelerating the rate of liquefaction. Such schemes certainly depolymerize the coal molecules into oil and asphaltene directly or indirectly through preasphaltene, but also accelerate the gas

formation through the hydrocracking of alkyl side-chains and naphthene rings. Thus, the optimum amount of donor exists to produce the maximum yield of oil plus asphaltene. The optimum amount may vary due to the coal, donor and reaction conditions which are all influential upon the participation extent of the schemes. The present study certainly indicates the optimum amount of the donor for the maximum yield. Taiheiyo coal required more donor for the production of oil than Morwell-I coal. Larger extent of depolymerization is required with higher rank coal.

The solvent is expected to play roles of dissolving and dispersing agents against coal-derived molecules and donor. Their intimate contact and radical dispersion which are strongly influential on the liquefaction as well as retrogressive reactions are assured by the solvent. Hence, the amount of non-donor solvent participates the liquefaction scheme. The difference between the same amounts of the donor in the fixed amount of aromatic solvent and alone without additional solvent is thus definite, although smaller amount of solvent may be favorable when the product slate is acceptable.

The optimum amount of donor can be reduced under the hydrogen pressure if the hydrogen is transferred to the donor, coal molecules or radicals derived from donor and coal molecules. Vernon has indicated the participation of molecular hydrogens in the pyrolysis[14]. The present results indicate that it is possible with certain types of model molecules and coals. Such a participation of molecular hydrogen under some pressures may reduce the difficulty of catalytic hydrotreating process of the second stage, where the hydrocracking for more oil and hydrogenation for the solvent regeneration are both expected. The first stage requires some pressure in any case to maintain the solvent in the liquid phase and coal-derived molecules.

The deashing for some coals has been reported to increase the yield of liquid product in the hydrogen transferring liquefaction with sufficient amount of solvent through enhanced fusibility via liberation of coal macromolecules[11]. It is not always the case when less amount of solvent is applied. Larger amount of donor may be necessary at a time to match the enhanced reactivity of deashed coal. Morwell-II coal exhibited certainly less reactivity and influence of deashing. The marked difference is found in the conversion of asphaltene to oil. More unreactive asphaltene is presented in the product from Morwell-II coal. Detail structure of asphaltene is an objective of future study. Taiheiyo coal exhibited little influence of deashing, especially with smaller amount of donor solvent.

The combination of deashing pretreatment and hydrogen pressure is of value for study to obtain higher yield of oil and asphaltene by reducing the preasphaltene and residue, since the deashing pretreatment is expected to simplify the liquefaction steps and solve the operational problems[18].

The amount of solvent can be hopefully reduced to the level which is necessary for coal slurry transportation, which requires a significant amount of liquid at room temperature. Such a vehicle solvent is not needed any more when a certain extent of liquefaction has proceeded to supply the solvent fraction. The

removal of such lightest portion in the solvent can economize the reactor volume.

References
1. Taunton,J.W., Trachte,K.L. and Williams,R.D., Fuel, 1981, 60, 788.
2. Weber,W. and Stewart,N., EPRI Journal, 1987, 12(1), 40.
3. Strobel,B.O. and Friedrich,F., Proc. Int. Conf. Coal Science, 1985, Sydney, p.7.
4. Okuma,O., Yanai,S., Mae,K., Saito,K. and Nakako,Y., Proc. Int. Conf. Coal Science, 1987, Maastricht, p.307.
5. Whitehurst,D.D., Fuel Process. Technol., 1986, 12, 299.
6. Kamiya,Y., Ohta,H., Fukushima,A., Aizawa,M. and Mizuki,T., Proc. Int. Conf. Coal Science, 1983, Pittsburgh, p.195.
7. Weller,S. and Pelipetz,M.G., I & EC Proc. Dev., 1951, 43(5), 1243.
8. Given,P.H. and Derbyshire,F.J., DOE-PC-60811-7,8, 1985, p.28.
9. Mochida,I., Otani,K., Korai,Y. and Fujitsu,H., Chem. Lett., 1983, 1025.
10. Mochida,I., Yufu,A., Sakanishi,K., Korai,Y. and Shimohara,T., J. Fuel Soc. Jpn., 1986, 65, 1020.
11 Mochida,I., Yufu,A., Sakanishi,K. and Korai,Y., Fuel, 1988, 67, 114.
12. McMillen,D.F., Ogier,W.C., Chang,S., Fleming, R.H. and Malhotra,R., Proc. Int. Conf. Coal Science, 1983, Pittsburgh, p.199.
13. Kamiya,Y., Futamura,S., Mizuki,T., Kajioka, M. and Koshi, K., Fuel Process. Technol., 1986, 14, 79.
14. Vernon,L.W., Fuel, 1980, 59, 102.
15. Mochida,I., Kishino,M., Sakanishi,K., Korai,Y. and Takahashi,R., Energy & Fuels, 1987, 1, 343.
16. Mochida,I., Shimohara,T., Korai,Y. and Fujitsu,H., Fuel, 1984, 63, 847.
17. Shimohara,T. and Mochida,I., J. Fuel Soc. Jpn., 1987, 66, 134.
18. Mochida,I., Sakata,R. and Sakanishi,K., Fuel in press.

Table 1

Elemental analyses of sample coals

Coal name	wt%(daf) C	H	N	(O+S)	Ash (wt%)
Morwell-I	60.5	5.5	0.5	33.4	2.4
Deashed-I	61.2	5.4	0.5	32.9	1.1
Morwell-II	63.7	4.9	0.6	30.8	2.3
Taiheiyo	73.5	6.3	1.2	19.0	17.3
Deashed coal	73.9	6.3	1.3	18.6	10.9

Table 2

Influences of donor(4HFL) concentration in the solvent[1] on the liquefaction yields from Morwell-I coal at 450 °C

4HFL	Reaction	Yield (wt%)				
(%)	time(min)	Gas	Oil	Asph.	Preasph.	Residue
100	5	19	56	13	12	0
	20	20	62	14	4	0
	30	28	53	14	5	0
75	5	13	51	15	15	6
	20	14	68	14	4	0
	30	13	68	14	5	0
50	5	6	50	23	14	7
	10	10	56	19	6	9
	30	9	60	22	6	3
25	5	8	44	21	12	15
	10	8	47	18	14	13
	30	10	48	17	7	18

1) Solvent/coal ratio = 3/1(fixed)
Solvent composition : 4HFL/(4HFL+FL)
(FL: fluoranthene, 4HFL: tetrahydro-FL)

Table 3

Influence of hydrogen pressure on dibenzyl(DB) conversion at 450 °C-30 min

Atmosphere[1]	Reactants (mmol)			Conversion(%)	
(kg/cm^2)	DB	FL	4HFL	DB	4HFL
N_2 (10)	2.75	14.9	0	25	-
H_2 (20)	2.75	14.9	0	36	-
N_2 (10)	2.75	14.6	0.24	25	100
H_2 (20)	2.75	14.6	0.24	33	76
N_2 (10)	2.75	14.4	0.49	32	85
H_2 (20)	2.75	14.4	0.49	38	58

1) ( ): initial pressure

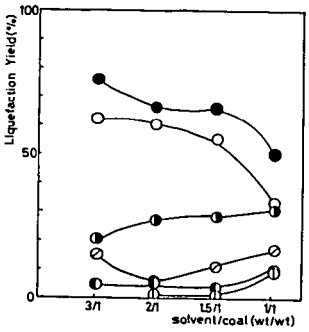

Fig.1
Influence of solvent(4HFL)/coal ratio on the liquefaction yields at 450°C
● :(oil+asphaltene), ○:oil, ◑:gas, ∅:asphaltene, ◐:preasphaitene, ⓓ:residue

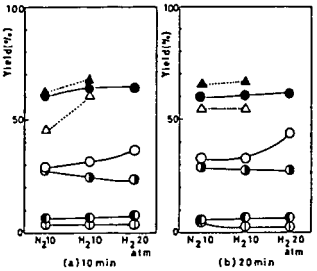

Fig.2
Effects of hydrogen pressure on the liquefaction of Morwell-I and -II coals at 450°C, 1.5/1(solvent/coal)
Morwell-I ▲:O+A, △:O
Morwell-II ●:O+A, ○:O, ◑:G, ◐:P, ⓓ:R

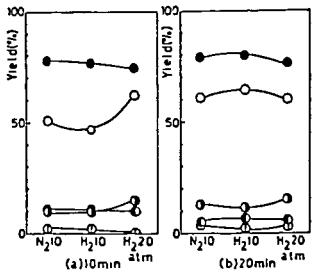

Fig.3
Effect of hydrogen pressure on the liquefaction of Taiheiyo coal at 450°C and 1.5/1(solvent/coal)
●:(O+A), ○: O, ◑: G, ◐: P, ⓓ: R

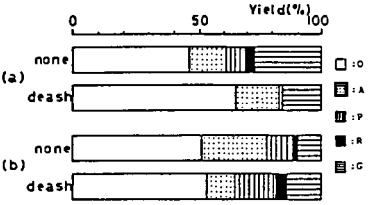

Fig.4
Effect of deashing on the liquefaction at 450°C-10 min(solvent/coal=1.5/1, solvent:4HFL)
(a) Morwell-I (b) Taiheiyo

CATALYTIC TWO-STAGE HYDROCRACKING OF ARABIAN VACUUM RESIDUE AT A HIGHER CONVERSION LEVEL WITHOUT SLUDGE FORMATION

Isao Mochida, Xing-zhe Zhao and Kinya Sakanishi

Institute of Advanced Material Study,
Kyushu University,
Kasuga, Fukuoka 816, JAPAN

ABSTRACT

Catalytic two-stage hydrocracking of Arabian vacuum residue was studied using commercial Ni-Mo catalysts in the autoclave to achieve a higher conversion above 50 % into 540 °C⁻ distillate without producing sludge in the product. The hydrogenation at 390 °C of the first stage was found very effective to suppress the sludge formation in the second stage of higher temperature, 430 °C, where the cracking to produce the distillate dominantly proceeded. The catalyst for the residues(KFR-10) was suitable for these purposes, while KF-842 catalyst, which exhibited excellent performance against coal liquid residues, failed to suppress the sludge formation. The shorter contact time of the second stage at a relatively higher temperature appears favorable to increase the conversion without producing the sludge. The mechanism of sludge formation in the hydrocracking process is rather comprehensibly discussed based on the previous and present results.

INTRODUCTION

Demand for clean distillate from the bottom of the barrel leads to severe hydrocracking of petroleum residues at higher temperatures[1]. The severe conditions cause problems of coke deposition on the catalyst and sludge formation in the product oil[2]. Such trouble makers of both carbonaceous materials, of which formation may be intimately related, shorten the life of the catalyst, plug transfer line and deteriorate the quality of the products[3].

Empirically, the dry sludge is believed to be produced when the conversion to the distillate is beyond a certain level(ca. 50 %) regardless of the catalyst and feedstocks[1]. Its structure, properties and formation mechanism are not fully understood yet[4].

In a previous study[5], dry sludge produced in a hydrocracked oil was analyzed chemically, and its solubility, fusibility and reactivity were studied to propose a mechanism of sludge formation in the hydrocracking process.

In the present study, catalytic two-stage hydrocracking was proposed to achieve a higher conversion into 540 °C⁻ distillate above 50 % with a minimum amount of dry sludge in the product. The idea is based on the mechanism previously proposed: the deep hydrogenation of aromatic fraction in the residue by the first stage of lower temperature may accelerate the cracking and solubility of the heaviest aromatic portion in the second stage of higher temperature, where major hydrocracking takes place.

EXPERIMENTAL

Materials

A vacuum residue (b.p.> 550 °C) of Arabian-light oil (10 g), of which properties were shown in Table 1, was hydrocracked by the single- and two-stage reactions under hydrogen pressure (15 MPa), using one of the Ni-Mo catalysts (1 g) in a batch autoclave of 100 ml capacity. The catalysts, of which properties were summarized in Table 2, were presulfided under 5 % H_2S/H_2 flow at 360 °C for 6 h.

Catalytic hydrocracking

The standard conditions were 390 °C-4 h, 420 °C-4 h for the single-stage reaction, and 390 °C-3 h(first stage) and 420 - 440 °C-1 h(second stage) for the two-stage reaction, respectively. No solvent was used except for the two-stage reaction of 390 °C-3 h and 440 °C-1 h; 10 wt% of 1-methylnaphthalene was added before the second stage for comparison with no-solvent reaction under the same conditions. After removal of the catalyst, the product was observed under a optical microscope to measure the amount of sludge in the product. The product was distilled under vacuum (5 mmHg) at 340 °C to obtain the distillate (540 $°C^-$ fraction) yield.

RESULTS

Single-stage hydrocracking

Table 3 summarizes the results of single-stage hydrocracking using two Ni-Mo catalysts. The reaction at 390 °C provided the yield of 540 $°C^-$ distillate below 50 %. No sludge was found with both catalysts at this temperature as shown in Figure 1a, where bluish spots of probably long-chain paraffins were observable, indicating insufficient extent of cracking. It is noted that the amount of asphaltene was unchanged after the hydrocracking at 390 °C.

Higher reaction temperature of 420 °C increased the distillate yield significantly above 70 %. However, a large amount of sludges was found with both catalysts as shown in Figures 1b and 1c. The appearances of the sludges were somewhat different with the catalysts; those with KF-842 consisted of black and rigid spheres and very fine brown oily-droplets, whereas those with KFR-10 were larger droplets which were brown and diffused. A significant amount of asphaltene was certainly converted under the conditions. It should be noted that KF-842 produced a significant amount of gaseous products at 420 °C. Thus, the catalysts, KF-842 for the distillate of coal liquid and KFR-10 for the petroleum straight residue behaved very differently against the petroleum residue.

Two-stage hydrocracking

Results of two-stage hydrocracking are summarized in Table 4. The two-stage hydrocracking using KF-842 at 390 °C-3 h and 420 °C-1 h still produced a very large amount of sludge in the product oil as shown in Figure 2a, although the distillate yield was still high. KFR-10 catalyst under the same conditions produced negligible amount of sludge as shown in Figure 2b at the distillate yield as high as 66 %. Longer reaction time of 3 h in

the second stage at 420°C increased slightly both sludge and the distillate yield(70 %).

Higher temperature of 440 °C for 1 h in the second stage increased the yield to 81 %, some sludgebeing produced as shown in Figure 2c.

Addition of 10 % 1-methylnaphthalene to the second stage at 440 °C was very effective to suppress the sludge formation (Figure 2d). The distillate yield was as high as 80 %.

Storage stability of hydrocracked product

The hydrocracked product obtained by the single stage of 420 °C-4 h using KF-842 catalyst was rather unstable. The product carried a small amount of sludge just after the reaction as shown in Figure 1b, however a much larger amount was found 150 days later in the same product(Figure 3). Insufficient hydrogenation or dehydrogenation because of high reaction temperature may leave unsaturated sites reactive for the air-oxidation. In contrast, no deterioration was observed with the products obtained by using KFR-10 catalyst under the same conditions and the two-stage reactions with either catalyst, although a large amount of sludge has been produced right after the two-stage hydrocracking with KF-842 catalyst.

DISCUSSIONS

Structure and formation mechanism of dry sludge in the hydrocracking

The hexane-soluble fraction (HS) in the hydrocracked product consists of essentially of long-chain paraffins and long alkylbenzenes. In contrast, the insoluble substances in the sludge are fairly aromatic with much less and shorter alkyl groups and rather polar, carrying a considerable amount of heteroatoms. The solubility decreased with increasing aromaticity and polarity, the molecular weight varying rather slightly among the fractions. Such contrast structural characteristics of HS and HI fractions may not allow their mutual miscibility, precipitating or segregating the insoluble substances from the HS matrix at room temperature.

In spite of low solubilities of the sludge components at room temperature, they melt or are dissolved in the light component at elevated temperatures above 80 °C. Thus, the sludge may disappear at elevated temperatures such as the reaction temperature, although its limited solubility in the matrix may enhance its adsorption or longer residence on the catalyst surface, leading to the severe catalyst deactivation.

Based on the analyses of the sludge, a mechanism of its formation is proposed[5]. Hydrocracking at higher temperatures to achieve a higher conversion can crack deeply the paraffinic and and alkyl aromatic hydrocarbons at a high level, however highly-condensed aromatic hydrocarbons are not fully hydrogenated at higher temperatures for their cracking because dehydrogenation is so rapid under the conditions, staying unchanged in their ring structure to be insoluble in the paraffin-rich matrix, especially at lower lower temperatures. Elimination of alkyl side-chains from aromatic hydrocarbons and severe cracking of light aromatic

hydrocarbons enhance the phase separation to lead to the sludge formation.

Such a mechanism originating from the phase separation of the fractions due to their mismatched compatibility appears to be common to bottom and shot cokes formation in the coking[6,7], and least cracking reactivity of paraffin[8-10] and sludge formation due to the slight oxidation in the coal liquid.

Effects of two-stage hydrocracking

The two-stage hydrocracking which consists of sufficient hydrogenation at a lower temperature and extensive cracking of the hydrogenated product at a higher temperature was found to allow a high yield of distillate over 60 % with a minimum amount of sludge droplets in the product at room temperature. As discussed in the mechanism section, the sludge was unhydrogenated aromatics due to high reaction temperature, which are not miscible with the paraffin-dominant matrix. The first stage of low temperature sufficiently hydrogenates the aromatic parts of the asphaltene to be easily cracked and/or to stay miscible with the matrix, increasing the yield of distillate without producing sludge in the second stage. Aromatic solvent of moderate size such as 1-methylnaphthalene is very effective in the second stage of the short reaction time to suppress the sludge by dissolving the asphaltene.

The selection of conditions for the second stage is very important because extensive cracking should take place before the dehydrogenation. Longer reaction time at higher temperature tends to produce more sludge because uncracked remaining asphaltene in the product becomes sludge. The rapid heating to the temperature of the second stage may be favorable.

The selection of the catalyst is also important. The catalyst should have strong hydrogenation activity against the asphaltene of large molecules. The large pores of the support can get access to such molecules. The catalyst of the second stage should have high cracking activity against the hydrogenated asphaltene without dehydrogenation.

Such a set of the catalysts should be designed separately to exhibit the optimum performances of the respective objectives at the respective stages.

Finally, the stability of hydrocracked product is concerned. The post-hydrogenation may be effective at a lower temperature, where sufficient hydrogenation of the whole product can proceed. Sludge can be completely removed by the step as described in a previous paper[5]. Short reaction time of the second stage can maintain the hydrogenation level high which is achieved in the first stage, proving the stability of the product.

References

1. Saito, K. and Shimizu,S., PETROTECH, 1985, 8(1), 54.
2. Symoniak,M.F. and Frost,A.C., Oil & Gas Journal, 1971, March 15, 76.
3. Mckenna,W.L., Owen,G.H. and Mettick,G.R., Oil & Gas journal, 1964, 62(20), 106.

4. Haensel,V. and Addison,G.E., Advances in Catalytic Reforming, 7th World Petroleum Congress, 1967, 4, 113.
5. Mochida,I., Zhao,X.Z. and Sakanishi,K., Ind. Eng. Chem. Res. in submission.
6. Mochida,I., Furuno,T., Korai,Y. and Fujitsu,H., Oil & Gas Journal, 1986, 3, 51.
7. Eser,S., Jenkins,R.G. and Derbyshire,F.J., Carbon, 1986, 24, 77.
8. Mochida,I., Sakanishi,K., Korai,Y. and Fujitsu,H., Proc. Int. Conf. Coal Science, 1985, Sydney, p.63.
9. Sakanishi,K., Zhao,X.Z., Fujitsu,H. and Mochida,I., Fuel Process. Technol., 1988, 18, 71.
10. Inoue,Y., Kawamoto,K., Mitarai,Y. and Takami,Y., Proc. Int. Conf. Coal Science, 1985, Sydney, p.193.

Table 1

Solubility[1] of Arabian-light vacuum residue (ALVR)

	wt%		
	HS	HI-BS	BI
ALVR	91	9	0

1) HS: hexane soluble
HI-BS: hexane insoluble-benzene insoluble
BI: benzene insoluble

Table 2

Some properties of the catalysts[1]

Catalyst name	Support	Metal(wt%) NiO	Metal(wt%) MoO_3	Surface area (m^2/g)	Pore volume (ml/g)	Mean pore diameter (Å)
KF-842	alumina	3.1	15	273	0.52	< 100
KFR-10	silica-alumina	1.0	5.0	147	0.71	168

1) Supplier: Nippon Ketjen Co.

Table 3

Catalytic performances in the single-stage hydrocracking of ALVR

Catalyst	Conditions (°C- h)	Recovery (wt%)	D.Y.[1] (%)	A.S.[2]
KF-842	390-4	95	39	tr.
	420-4	75	72	much
KFR-10	390-4	98	41	tr.
	420-4	91	74	much

1) D.Y.: 540 °C⁻ distillate yield
2) A.S.: Amount of sludge, tr.: trace

Table 4

Catalytic performances in the two-stage hydrocracking of ALVR

Catalyst	Conditions (°C- h)	Recovery (wt%)	D.Y.[1] (%)	A.S.[2]
KF-842	390-3 420-1	94	63	much
KFR-10	390-3 420-1	94	66	v.tr.
	390-3 420-3	94	70	tr.
	390-3 440-1	93	81	some
	390-3 440-1[3]	95	81	v.tr.

1) and 2): See Table 3., v.tr.: very trace
3) 10 wt% of 1-methylnaphthalene was added prior to the second stage.

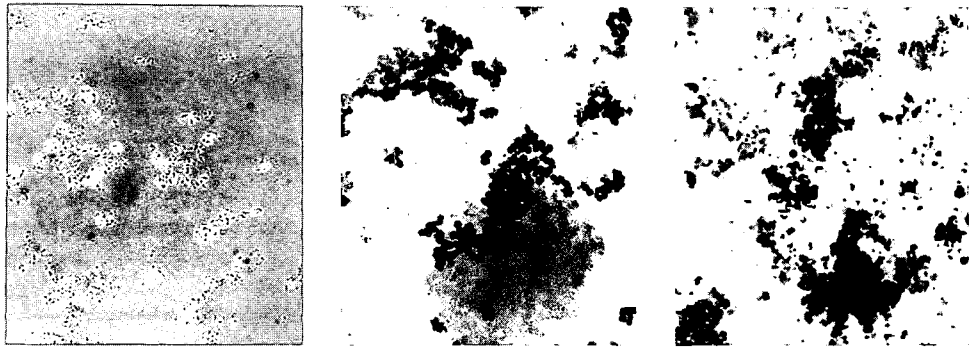

(a) (b) (c)

Figure 1 Microphotographs of the product oil in the single-stage reactions
(a) 390 °C-4 h (either catalyst)
(b) 420 °C-4 h (KF-842 catalyst)
(c) 420 °C-4 h (KFR-10 catalyst)

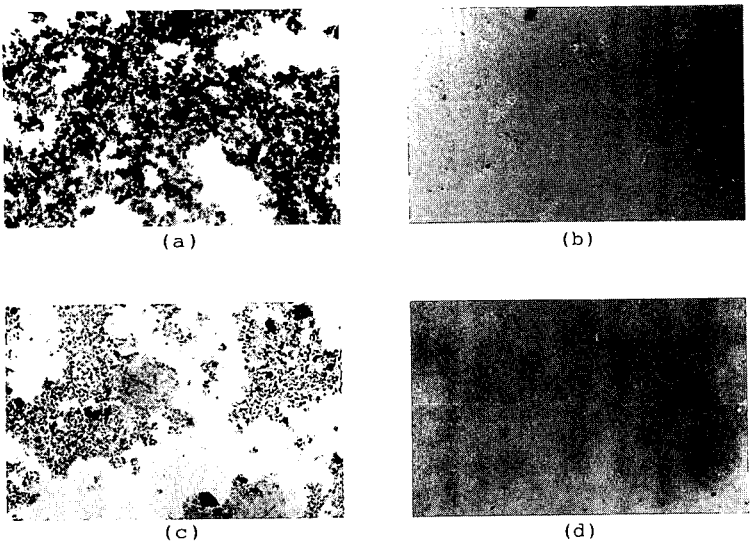

Figure 2 Microphotographs of the product oil in the two-stage reaction
(a) 390 °C-3 h and 420 °C-1 h (KF-842 catalyst)
(b) 390 °C-3 h and 420 °C-1 h (KFR-10 catalyst)
(c),(d): 390 °C-3 h and 440 °C-1 h (KFR-10 catalyst)
(c) no solvent added
(d) 10 wt% of 1-methylnaphthalene added in the second-stage reaction

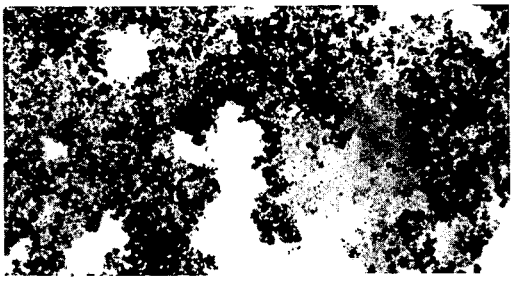

Figure 3 Microphotographs of the product of 420 °C- 4 h (KF-842) after 150 days